8-2022

An Evaluation of Castor californicus and Implications for the Evolution and Distribution of the Genus Castor (Rodentia: Castoridae) in North America

Kelly Lubbers
East Tennessee State University

An Evaluation of *Castor californicus* and Implications for the Evolution and Distribution of the Genus *Castor* (Rodentia: Castoridae) in North America

A thesis

presented to

the faculty of the Department of Geosciences

East Tennessee State University

In partial fulfillment

of the requirements for the degree

Master of Science in Geosciences, Paleontology

by

Kelly E. Lubbers

August 2022

Joshua X. Samuels, PhD, Chair

Blaine W. Schubert, PhD

T. Andrew Joyner, PhD

Keywords: Beaver, *Castor californicus*, *Castor canadensis*, Geometric Morphometrics, Ecological Niche Modeling, Conservation Paleobiology

ABSTRACT

An Evaluation of *Castor californicus* and Implications for the Evolution and Distribution of the Genus *Castor* (Rodentia: Castoridae) in North America

by

Kelly E. Lubbers

The genus *Castor* is represented in Eurasia by *Castor fiber*, North America by *C. canadensis*, and has been in North America since the late Miocene. This study aims to assess whether morphology of Miocene-Pliocene *C. californicus* and extant *C. canadensis* are distinctly different. Specimens of *Castor* were compared using geometric morphometrics on cranial material and linear measurements of postcranial material. Species occurrence data were compared with past and future climate data to assess *Castor* distribution in North America through time. Results show that *C. canadensis* is highly variable in both cranial and postcranial morphology and *C. californicus* falls largely within the range of variation seen within the extant species. Past distributions match fossil occurrences of *Castor*, suggesting confidence in projected models. Morphological and distribution similarities between the two species suggest that they can be treated as ecological analogs, though evaluation of whether they are conspecific will require more data.

DEDICATION

I would like to dedicate this project to my best friend, Reid Cummins. Without you, I wouldn't be where I am today. Thank you for all the years of friendship, encouragement, and pushing me to do my best. I only wish you could see where it has led me today.

ACKNOWLEDGEMENTS

I would sincerely like to thank the members of my committee, Dr. Josh Samuels, Dr. Andrew Joyner, and Dr. Blaine Schubert. I would also like to thank the Gray Fossil Site & Museum collections crew, especially Season Nye, Matt Inabinett, Sarah Clark, and Stokke Xu for their constant support and providing me with more opportunities for professional growth and learning. I'd also like to thank my roommates Darian Bouvier and Gus for their constant moral support and company. Also, I'd like to thank my fellow graduate students for helping be a good support system both online and in person these past two years. And lastly, I'd like to thank all my family, friends, and my two kitties back home, Geralt and Ciri, for all of their love and support.

TABLE OF CONTENTS

LIST OF TABLES

LIST OF FIGURES

CHAPTER 1. INTRODUCTION

Extant Beavers

Beavers are large, semiaquatic rodents notable for their thick fur, large webbed hind feet and broad, dorsoventrally flattened tail (Howell 1930; Long 2000). Beaver fur is composed of two types of hair, the long coarse guard hair and the soft short underfur (Jenkins and Buscher 1979; Muller-Schwarze 2011). This hair combination creates a dense fur which helps the beaver by retaining heat, repelling water, and staying buoyant (Muller-Schwarze 2011; Brazier et al. 2020). Beavers primarily propel themselves through the water with their webbed hind feet (Jenkins and Buscher 1979). Their tail helps propel them through the water, stabilize themselves when on land, communicate, and deter potential predators by slapping the surface of the water (Jenkins and Buscher 1979; Long 2000). Other methods of beaver communication include vocalization and scent marking (Jenkins and Buscher 1979). To mark their territory, beavers secrete a substance called castoreum which they produce through specialized castor glands (Long 2000; Brazier et al. 2020).

Castor canadensis is one of two extant members of the genus *Castor*, the other being *C. fiber*. Although the two species are similar in morphology, they are genetically and chromosomally different (*C. canadensis* 2n=40, and *C. fiber* 2n=48) (Jenkins and Buscher 1979; Rosell et al. 2005; Brazier et al. 2020). *Castor canadensis* has a distribution extending throughout North America (Figure 1), excluding the northern tundra, the Florida peninsula, and the southwest deserts (Jenkins and Buscher 1979). Within North America, *C. canadensis* occupies a diverse set of ecological regions (Naiman et al. 1988; Rosell et al. 2005). Their diets consist predominantly of softer wood trees, shrubs, and riparian vegetation (Jenkins and Buscher

1979; Long 2000). Tree preference includes aspen, willow, and alder, but they will also consume bark, twigs and leaves of other woody plants (Jenkins and Buscher 1979; Long 2000).

Figure 1. North American distribution of *Castor canadensis* (after Hall, 1981 and Peck, 2006)

Predators of *Castor canadensis* include wolves, coyotes, black bears, and cougars (Jenkins and Buscher 1979; Long 2000; Muller-Schwarze 2011). Birds, including hawks and owls, may also hunt smaller beavers (Long 2000). Alligators have also been known to hunt beavers in southern regions of North America, which may explain the absence of beavers in areas like peninsular Florida (Long 2000; Muller-Schwarze 2011). *Castor canadensis* is a dam building beaver, preferring to build its dam in streams and on the edge of ponds and lakes (Naiman et al. 1988; Wright et al. 2002; Rosell et al. 2005; Touihri et al. 2018). Dams are

typically built along first through fourth level streams (Naiman et al. 1988; Rosell et al. 2005). These dams significantly alter the ecosystem by blocking water flow which retains sediments and floods the surrounding area, providing ample space for beavers to hide from predators and gain access to additional food resources (Naiman et al. 1988). Beavers are often referred to as "ecosystem engineers" because of the impacts dam building has on modifying an ecosystem (Naiman et al. 1988; Wright et al. 2002; Rosell et al. 2005; Touihri et al. 2018).

Dam building impacts an ecosystem in multiple ways. Water drainage is highly reduced because of increased sediment accumulation, which alters the carbon and nitrogen budgets in the ecosystem and reduces erosion and flooding (Naiman et al. 1988; Rosell et al. 2005). Water quality improves as surface water and groundwater can interact with the heightened water table (Rosell et al. 2005; Touihri et al. 2018). Vegetation changes as previously tree covered areas are cut down and replaced by smaller grasses and shrubs along riparian zones (Naiman et al. 1988; Wright et al. 2002). Biodiversity also increases as invertebrate communities thrive in the low energy wetlands (Naiman et al. 1988).

Prior to European settlement, *Castor canadensis* populations were estimated to be over sixty million in North America (Naiman et al. 1988; Dolin 2011). However, *C. canadensis* was hunted by the fur trade as their pelts and castoreum were highly sought after (Naiman et al. 1988; Rosell et al. 2005). By the early 1800s, beaver populations significantly decreased on the east coast and expeditions ventured westward in search of more beavers (Naiman et al. 1988). By 1900, *C. canadensis* populations in North America were in danger of becoming extinct (Jenkins and Buscher 1979; Naiman et al. 1988; Rosell et al. 2005).

In the 1920s, both *C. canadensis* and *C. fiber* were protected by law and reintroduced through specialized programs (Rosell et al. 2005). Since then, populations of *C. canadensis* in

North America have significantly rebounded to an estimated population between ten and fifteen million (Naiman et al. 1988; Rosell et al. 2005; Muller-Schwarze 2011; Pollock et al. 2017).

Beaver-altered ecosystems play an important role in species and ecosystem conservation and are often a valuable resource for conservation management (Rosell et al. 2005; Pollock et al. 2017). With increased wildlife-urban interface and climate change, the impacts of beaver dam building could have increased effects on humans, potentially costing millions of dollars per year (Thompson et al. 2020). By understanding the ecological benefits provided by beavers, conservation efforts can be better understood and funded.

Fossil Record of Beavers

Beavers (Family Castoridae) first appeared in North America during the late Eocene and from there dispersed into Eurasia (Korth 1994; Flynn and Jacobs 2008). The fossil record of beavers includes approximately 30 genera, with diverse lineages adapted for fossorial, terrestrial, and semiaquatic lifestyles (Martin and Bennett 1977; Martin 1989; Korth 1994; Rybczynski 2007; Samuels and Van Valkenburgh 2008; Samuels and Van Valkenburgh 2009). The semiaquatic lineage of beavers, consisting of both Castorinae and Castoroidinae, diversified in the Miocene (Rybczynski 2007; Rybczynski et al. 2010). The genus *Castor* likely appeared in the late Miocene, as represented by *Castor neglectus* from Germany (Hugueney 1999; Flynn and Jacobs 2008). Little is known about the dispersals of *Castor* between North America and Eurasia, though it is likely those migrations were facilitated using the Bering land bridge throughout the Cenozoic (Rybczynski 2007; Flynn and Jacobs 2008; Samuels and Zancanella 2011).

Castor has been present in North America since the late Miocene, around 7 million years ago (Samuels and Zancanella 2011). *Castor californicus* was first discovered in the Kettleman Hills in California (Kellogg 1911). Kellogg (1911) designated it as a separate species from *C. canadensis* based on upper 3rd molar (M3) dental features, including a greater anteroposterior diameter and three enamel folds (striations) along the outer tooth wall. Other specimens of *C. californicus*, including cranial, postcranial, and dental material, have been discovered and described in Miocene and Pliocene localities across the western United States, including Idaho, Oregon, and Nebraska (Zakrzewski 1969; Shotwell 1970; Kurten and Anderson 1980; Samuels and Zancanella 2011). Specimens described as *Castor californicus* show only subtle differences in tooth morphology from extant North American beavers (Kellogg 1911; Stirton 1935). A second species of fossil beaver in North America, *Castor accessor*, was initially described by Hay in 1927 and designated as a separate species based on differences in striae lengths compared to *C. californicus* and *C. canadensis* (Hay 1927; Kurten and Anderson 1980). Hay (1927) confined the species to the late Blancan through the late Irvingtonian. However, due to similarities between size and temporal distribution, *C. accessor* is generally combined with *C. californicus* (Stirton 1935; Flynn and Jacobs 2008).

Castor specimens from the Miocene and Pliocene of North America have been referred to as *C. californicus*, while those from the Pleistocene to recent are referred to the living species *C. canadensis* (Kurten and Anderson 1980; Flynn and Jacobs 2008). From the Miocene through the Pleistocene of North America, *Castor* seems to have gotten slightly smaller (Stirton 1935; Shotwell 1970), but otherwise changed little morphologically (Martin 1989; Samuels and Zancanella 2011). That raises the question of whether the two species are distinct or represent change in a single species over time.

The purpose of this study is to evaluate whether the Miocene-Pliocene *C. californicus* and the Pleistocene and extant *C. canadensis* are distinctly different. This will improve understanding of *Castor* in North America over time and help resolve whether the two species can be treated as ecological analogs. The second portion of this study examines the distribution of *Castor* in the past and at present in order to help predict the potential future range in the face of climate change. Historically, *C. canadensis* could be found across most of North America, and *Castor* fossils are broadly distributed in the Pliocene and Pleistocene.

This study can help improve the understanding of the evolution of modern beavers and provide a better time resolution for dispersal of *Castor* across North America. Since beavers are ecosystem engineers, they significantly impact their surrounding ecosystem by altering geomorphology of watersheds and increasing biodiversity (Naiman et al. 1988; Wright et al. 2002; Rosell et al. 2005; Touihri et al. 2018). Beavers are also one of the great conservation success stories, but like many other organisms their future survival is uncertain due to anthropogenically driven climate change and habitat destruction (Naiman et al. 1988; Rosell et al. 2005; Pollock et al. 2017; Touihri et al. 2018; Thompson et al. 2020). Understanding past distributions could help piece together the ecological ranges of these organisms, which with climate data could help predict future ranges. Information yielded from this study could then help inform future conservation efforts.

CHAPTER 2. METHODS

Institutional Abbreviations

ETMNH-Z, East Tennessee State University Museum of Natural History Zoology Collection (Johnson City, TN, USA); FMNH, Field Museum of Natural History (Chicago, IL, USA); HAFO, Hagerman Fossil Beds National Monument (Hagerman, Idaho, USA); IMNH, Idaho Museum of Natural History (Pocatello, Idaho, USA); LACM, Los Angeles County Museum of Natural History (Los Angeles, California, USA); MVZ, University of California Berkley Museum of Vertebrate Zoology (Berkley, California, USA); UCLA, University of California Los Angeles (Los Angeles, California, USA); UF, Florida Museum of Natural History (Gainesville, Florida, USA); UOMNH, University of Oregon Museum of Natural and Cultural History (Eugene, Oregon, USA); USNM, Smithsonian Institution National Museum of Natural History (Washington D.C., USA); UWBM, University of Washington Burke Museum (Seattle, Washington, USA).

Geometric Morphometrics

Specimens

A total of sixty-seven specimens were used in the analysis of cranial material (Appendix A). Four specimens of *Castor fiber*, and fifty-nine of *Castor canadensis* accounted for the modern cranial samples. For the fossil specimens, three *Castor californicus* (HAFO 2243, UF 22520, USNM 26154), and one Pleistocene *Castor fiber* (FMNH 1537) were used.

Forty dentaries of both fossil and modern species were also used for this study (Appendix B). Modern specimens included two *Castor fiber* and thirty-five *Castor canadensis.* Fossil

specimens included two specimens of *Castor californicus* (UF 22520, USNM 26154) and one *Castor accessor* (UO 16338), which was classified as analogous to *Castor californicus*.

To minimize the effects of allometry, only adult specimens were used in the analysis. Adults were selected based on the level of fusion of the suture between the basioccipital and basisphenoid following Roberson and Shadle (1954).

Photographs and Landmark Placement

Cranial material was photographed in dorsal, lateral and ventral views, while dentaries were photographed in both lateral and medial views. In dorsal and ventral view specimens were photographed with the palate parallel to the photographic plane, and in lateral view the midline of the palate was aligned perpendicular to the photographic plane. The dentary was photographed with the occlusal surface of the cheek teeth aligned perpendicular to the photographic plane. Images were taken using a digital camera and saved to JPEG format. Thin-plate spline (TPS) files were created for all image views using the program tpsUtil32 (v.1.61), in preparation for landmark digitization (Rohlf 2015). The program tpsDig2 (v. 2.31) was used for digital placement of landmarks on specimen images (Rohlf 2021). Landmark placement for cranial material followed those previously used in Samuels and Van Valkenburgh (2009) and dentary landmarks followed those previously used in Monteiro et al. (2005). Table 1 and Figure 2 highlight the landmarks and placement used for cranial material, while Table 2 and Figure 3 highlight those used for the dentary. To minimize the potential effects of asymmetry, one side was used for the dorsal and ventral cranial views.

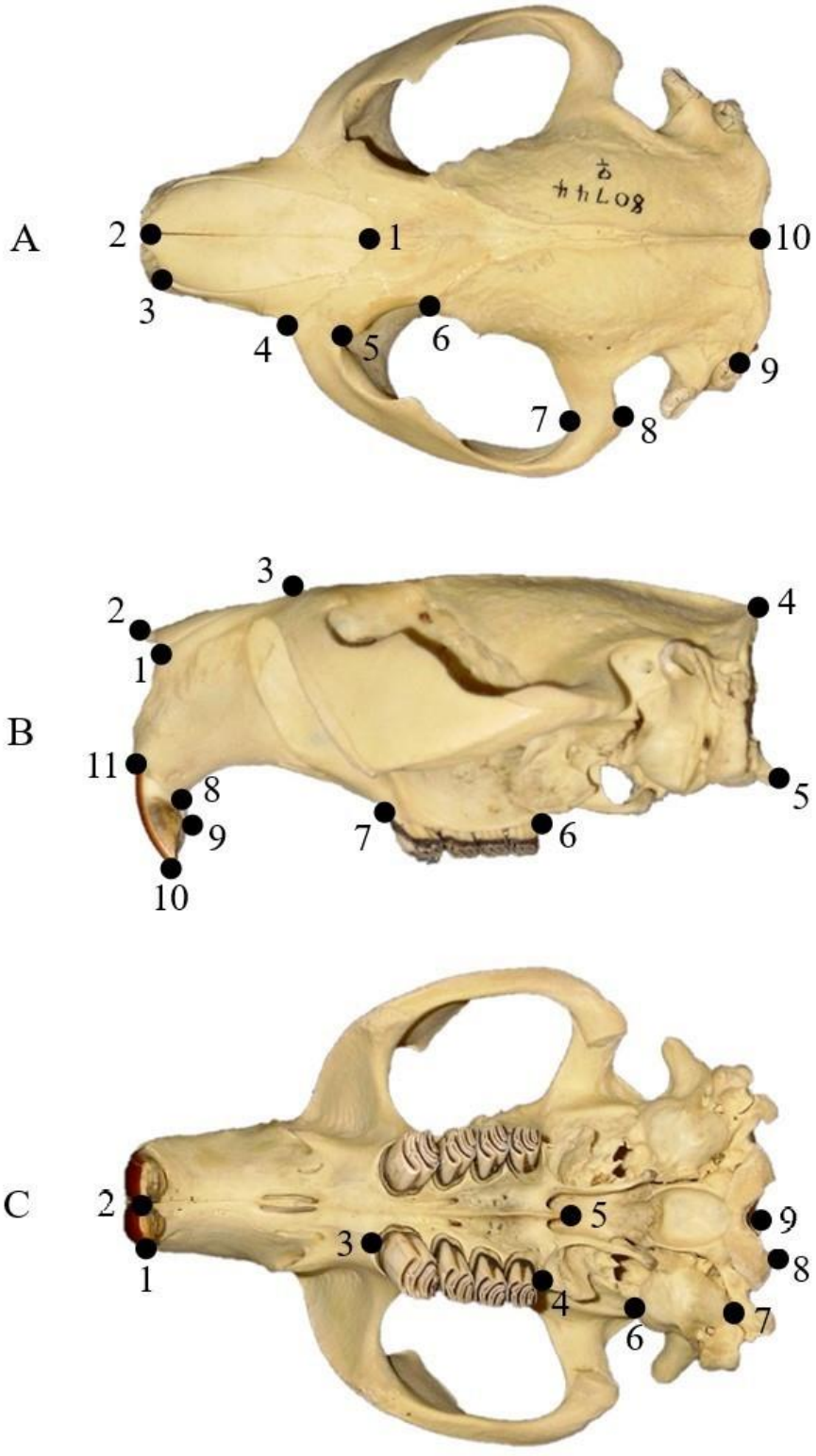

Figure 2. Landmark placement for dorsal (A), lateral (B), and ventral (C) views on *Castor canadensis* MVZ 80744. Descriptions of landmarks are outlined in Table 1

Table 1. Landmark number and description correlating for each view following Samuels and Van Valkenburgh 2009

Cranium Dorsal View	
Landmark #	Placement Description
1	Meeting point between nasal and frontal along midsagittal plane
2	Anterior tip of nasal along mid sagittal plane
3	Anterior tip of suture between nasal and premaxilla
4	Anterior tip of suture between premaxilla and maxilla
5	Posterior tip of suture between frontal and jugal
6	Postorbital constriction
7	Most posterior point of temporal fossa along squamosal process of the zygomatic arch
8	Most posterior meeting point between jugal and squamosal process of zygomatic arch
9	Y shaped suture at meeting point of squamosal, parietal, and occipital
10	Most posterior meeting point of sagittal and nuchal crests
Cranium Lateral View	
Landmark #	Placement Description
1	Anterior tip of suture between nasal and premaxilla
2	Anterior tip of nasal
3	Meeting point of nasal and frontal along the midsagittal plane
4	Most posterior meeting point of sagittal and nuchal crests
5	Most posterior point of occipital condyle
6	Posterior end of cheek tooth row
7	Anterior end of cheek tooth row
8	Most posterior point of incisor alveolus
9	Posterior edge of upper incisor blade
10	Anterior edge of upper incisor blade
11	Most anterior point of upper incisor alveolus
Cranium Ventral View	
Landmark #	Placement Description
1	Lateral edge of upper incisor blade
2	Medial edge of upper incisor blade
3	Anterior end of cheek tooth row
4	Posterior end of cheek tooth row
5	Posterior tip of palate along midsagittal plane
6	Most lateral point of suture between tympanic and squamosal
7	Suture where tympanic and occipital meet
8	Most posterior point of occipital condyle
9	Midsagittal border of foramen magnum

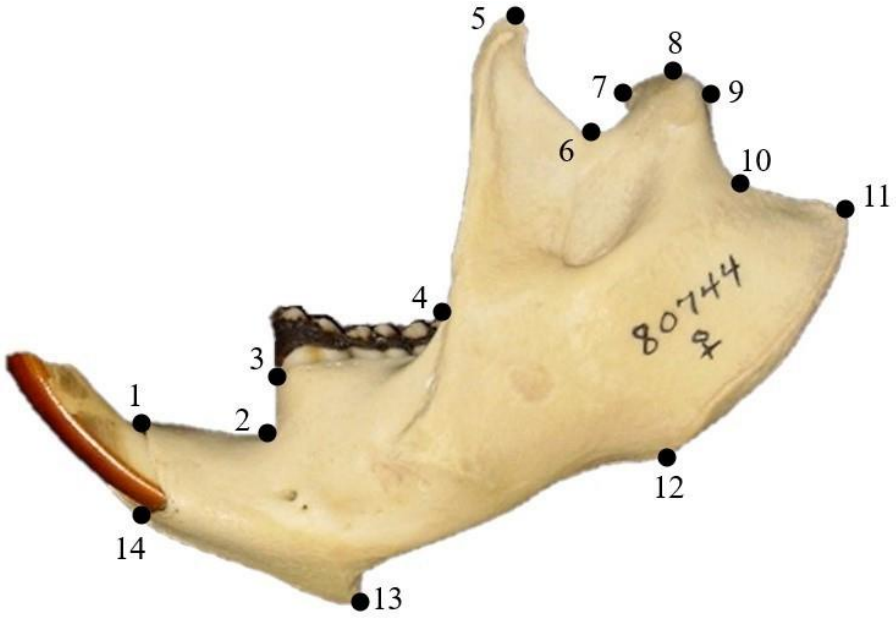

Figure 3. Landmark placement for dentaries. Specimen in image *Castor canadensis* MVZ 80744 in lateral view. Definitions of landmarks outlined in Table 2

Table 2. Landmark number and description correlating for each view following Monteiro et al. 2005

Dentary Landmarks	
Landmark #	Placement Description
1	Antero-dorsal boarder of incisive alveolus
2	Extreme of diastema invagination
3	Anterior edge of molar tooth row
4	Posterior intersection of molar tooth row with coronoid process
5	Tip of coronoid process
6	Maximum curvature between the coronoid and condylar processes
7	Anterior edge of articular surface of condyle
8	Tip of condylar process
9	Posterior most edge of articular surface of condyle
10	Maximum curvature on the curve between the condylar and angular processes
11	Tip of the angular process
12	Anterior margin of the angular process
13	Posterior extremity of the mandibular symphysis
14	Antero-ventral border of the incisive alveolus

Data Analysis

Landmark data were first analyzed via Relative Warp Analysis (RWA). The RWA used generalized least square Procrustes analysis to scale, rotate, and align coordinate sets assigned by landmark placement. A consensus configuration was generated from landmark coordinates from all specimens in each view to determine the average shape. Partial warp scores and uniform components were then determined based on variations from the consensus configurations. Differences in shape were marked by deformations within a grid, modeled and computed using thin-plate splines. The weight matrix (containing the partial warp scores and uniform components), centroid size, and relative warp scores for each view were calculated and downloaded from the tpsRelw program (v 1.70) (Rohlf 2015).

Relative warp analysis (RWA), which is like a principal component analysis (PCA), was conducted to understand the morphological variation separating individual specimens included in the study (Zelditch et al. 2004). Relative warps were calculated from the bending energy required to modify the consensus into a modified configuration based on morphological changes in specimens for each view. The RWA was completed in tpsRelw (Rohlf 2015).

Two subsequent analyses were conducted using the resulting warp scores produced from the landmark data. Those analyses included stepwise canonical variates analysis (CVA) and hierarchical cluster analysis. All tests were conducted on specimen landmark data for dentary material and the dorsal, lateral, and ventral views of the cranium.

Stepwise canonical variate analysis (CVA) was conducted in order to understand the morphological variation present among groups (Zelditch et al. 2004). Two CVAs were run using partial warp scores and uniform component scores produced from landmark data. Both cranial and dentary analyses were run separately. Partial warp scores and uniform component scores

were used as variables for the analyses. The first CVA used both *Castor canadensis* and *Castor fiber* as *a priori* categories with *Castor californicus* classified as unknown for the analysis to determine group placement. The second CVA categorized all three species individually into *a priori* categories. CVA was run in SPSS 26.0 and shapes associated with CV scores visualized with tpsRegr (Rohlf 2011).

The hierarchical cluster analysis was run to examine the phenetic relationship between specimens based on their morphology, without the need for *a priori* grouping of species. The cluster analysis was run in SPSS 26.0 using an unweighted pair group method with partial warp scores and uniform component scores.

Postcranial Analysis

Specimens

The analysis of postcranial material used a total of fifty-nine individuals (Appendix C). Modern specimens included thirty *Castor canadensis* and two *Castor fiber*. Fossils were composed of twenty-six specimens previously identified as *Castor californicus*. Sixty-four postcranial characteristics were recorded, measuring features including total lengths of bones, midshaft diameters, prominent articular surfaces and features. Measurements were collected in millimeters (to 0.01 mm) using Mitutoyo digital calipers. The list of measurements used for this portion of the analysis is listed in Table 3.

Table 3. Measurements of post cranial elements, following Samuels and Van Valkenburgh 2008

Measurement	Definition
ScaL	Length of scapula
ScaW	Width of scapula
ScaAL	Length of acromion process of the scapula
HL	Length of humerus
HAPD	Anteroposterior diameter of humerus
HMLD	Mediolateral diameter of humerus
HHD	Diameter of humeral head
HDAW	Articular width of humeral distal end
RL	Length of radius
RAPD	Anteroposterior diameter of radius
RMLD	Mediolateral diameter of radius
UL	Length of ulna
UAPD	Anteroposterior diameter of ulna
UMLD	Mediolateral diameter of ulna
ULOL	Length of olecranon process of the ulna
MC1L	Length of 1st metacarpal
MC2L	Length of 2nd metacarpal
MC3L	Length of 3rd metacarpal
MC3APD	Anteroposterior diameter of 3rd metacarpal
MC3MLD	Mediolateral diameter of 3rd metacarpal
MC4L	Length of 4th metacarpal
MC5L	Length of 5th metacarpal
Mph3p	3rd manus proximal phalanx
Mph3m	3rd manus medial phalanx
Mph3t	3rd manus terminal phalanx
InnomL	Length of innominate (ilium to ischium)
IllL	Length of ilium
FeL	Length of femur
FeAPD	Anteroposterior diameter of femur
FeMLD	Mediolateral diameter of femur
FeGT	Height of greater trochanter of the femur
FeHD	Diameter of femoral head
FeEB	Femoral epicondylar breadth
TL	Length of tibia
TAPD	Anteroposterior diameter of tibia
TMLD	Mediolateral diameter of tibia
TPEAPD	Anteroposterior diameter of tibia proximal epiphysis

TPEMLD	Mediolateral diameter of tibia proximal epiphysis
TDEAPD	Anteroposterior diameter of tibia distal epiphysis
TDEMLD	Mediolateral diameter of tibia distal epiphysis
TLOF	Tibia length of fusion to fibula
FibL	Length of fibula
FibAPD	Anteroposterior diameter of fibula
FibMLD	Mediolateral diameter of fibula
CalcL	Length of calcaneus
CalcTL	Length of calcaneus tuberosity
MT1L	Length of 1st metatarsal
MT1APD	Anteroposterior diameter of 1st Metatarsal
MT1MLD	Mediolateral diameter of 1st metatarsal
MT2L	Length of 2nd metatarsal
MT2APD	Anteroposterior diameter of 2nd metatarsal
MT2MLD	Mediolateral diameter of 2nd metatarsal
MT3L	Length of 3rd metatarsal
MT3APD	Anteroposterior diameter of 3rd metatarsal
MT3MLD	Mediolateral diameter 3rd metatarsal
MT4L	Length of 4th metatarsal
MT4APD	Anteroposterior diameter of 4th metatarsal
MT4MLD	Mediolateral diameter of 4th metatarsal
MT5L	Length of 5th metatarsal
MT5APD	Anteroposterior diameter of 5th metatarsal
MT5MLD	Mediolateral diameter of 5th metatarsal
Pph3p	3rd pes proximal phalanx
Pph3m	3rd pes medial phalanx
Pph3t	3rd pes terminal phalanx

Analyses

Measurement data were input to SPSS 26.0 where descriptive statistics were run for each species. The analysis computed mean, standard deviation, and minimum and maximum values for the measurements of each species. From those data, coefficients of variation were calculated for each measurement across species. Coefficients of variation compare the range of variation seen within groups, in this case species, for various postcranial measurements. Coefficients of variation (CoVar) are calculated by the equation:

$$CoVar = \frac{\sigma}{\mu}$$

where σ represents sample standard deviation and μ represents sample mean. Only species measurements with more than three samples were used to calculate CoVar, as fewer than three would result from insufficient sampling. In addition to the descriptive statistics, an analysis of variance (ANOVA) was run for each of the measurements allowing assessment of differences in mean values between species groups.

Ecological Niche Modeling

Ecological niche models can be a useful tool to determine habitat suitability and species distributions (Davis et al. 2014; McGuire and Davis 2014). These models can be beneficial for understanding species ecological needs and potential distribution, and can assist with conservation management by identifying where to allocate and prioritize conservation resources (Botkin et al. 2007; McGuire and Davis 2014). Using both past and future bioclimatic data, with the recent fossil record, can help estimate habitat suitability and changes to it over time (Davis et al. 2014; McGuire and Davis 2014; Warren and Siefert 2011). The purpose of this portion of the study is to use species occurrence data along with bioclimatic variables to create models projecting the past, present, and future distributions and habitat suitability of *Castor* across North America.

Species Occurrence Data

Specimen occurrence data for *Castor canadensis* were downloaded from the Global Biodiversity Information Facility (GBIF). Point data for *C. canadensis* were used because of its

abundance and wide distribution across North America, which is readily available and allows high resolution comparisons with modern climate data. To best model a pre-bottleneck, before European settlement and widespread North American fur trapping, species distribution occurrence data included modern, historic, and Holocene records. *C. canadensis* data points falling outside of its known North American distribution and lacking coordinate data were removed from the dataset. Point data was spatially rarefied to one km using Species Distribution Model (SDM) toolbox in ArcGIS Pro 2.7.0 (Environmental Systems Research Institute (ESRI), Redlands, CA, USA) (Brown et al. 2017).

Fossil locality data for *C. californicus* and *C. canadensis* were used as validation points for the projection models. Fossil locality data for *C. californicus* were obtained from the Paleobiology Database (Figure 4) and *C. canadensis* data were obtained from the Neotoma database (Figure 5) and were spatially rarefied. One record for the late Miocene *C. californicus* specimen from the Rattlesnake Formation in Oregon was added as it was not included in the original Paleobiology Database dataset (Samuels and Zancanella 2011).

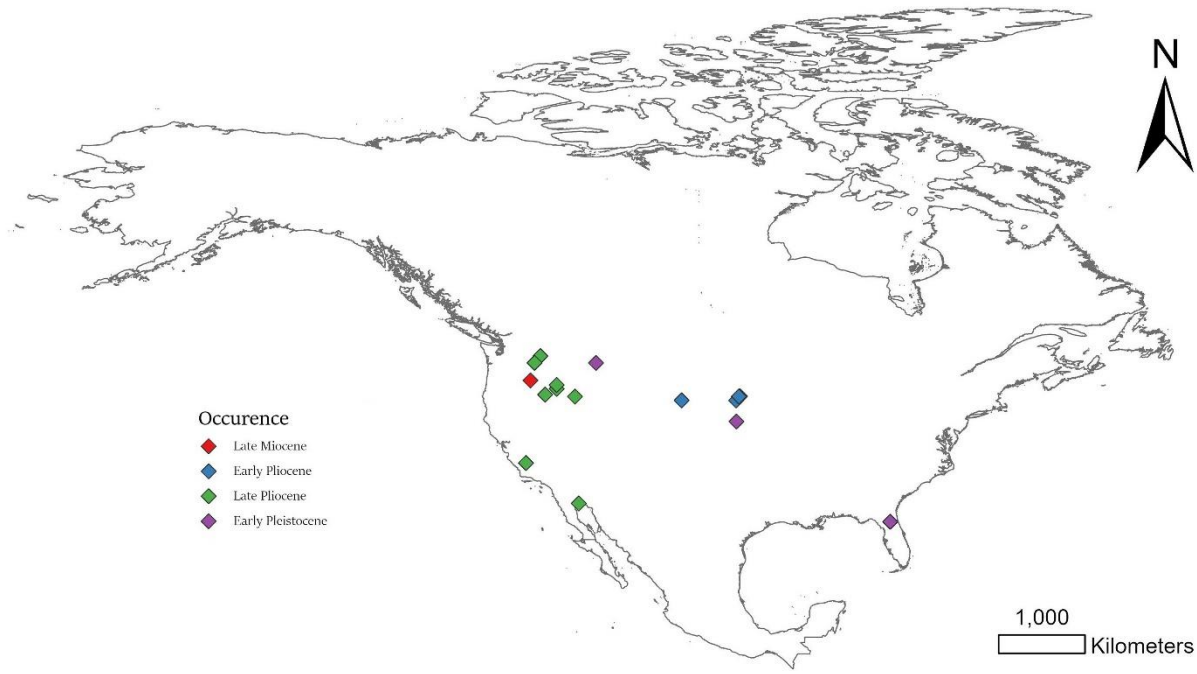

Figure 4. Distribution of fossil localities (Late Miocene to Early Pleistocene) of *Castor californicus* across North America

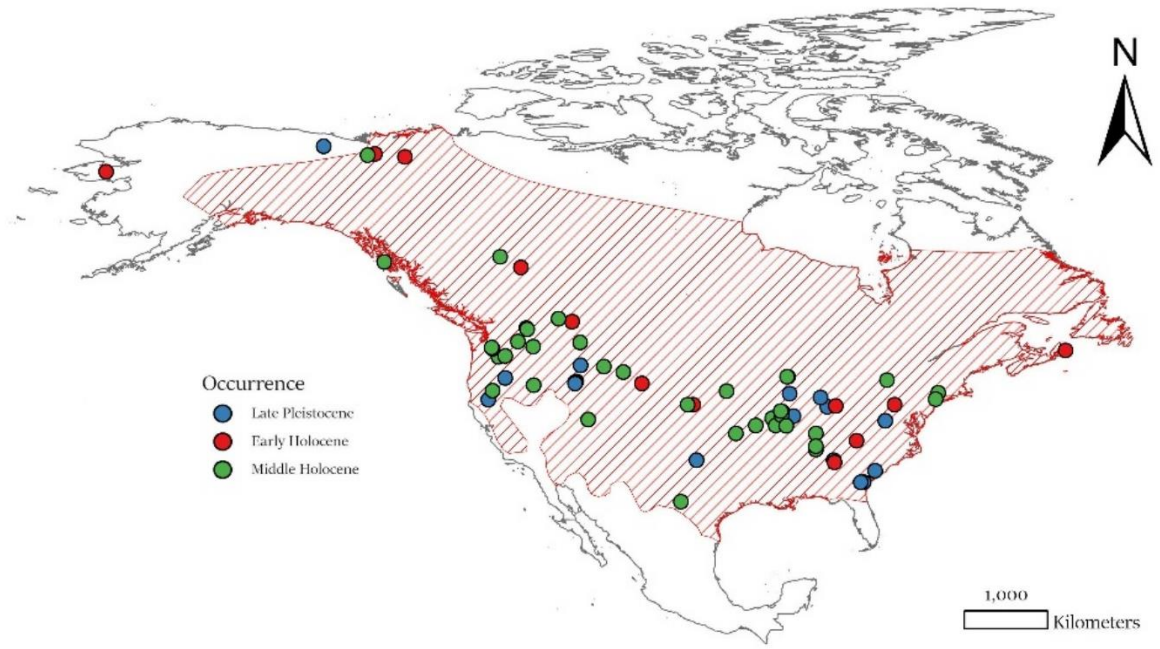

Figure 5. Distribution of fossil localities (Late Pleistocene to Middle Holocene) of *Castor canadensis* across North America. Red crosshatching represents the historic distribution of *C. Canadensis* (Hall 1981; Peck 2006)

Climate Data and Variables

Modern bioclimatic data (1970-2000) were downloaded from WorldClim (Fick and Hijmans 2017). These bioclimatic variables were downloaded at 2.5 min resolution, which equates to roughly five km of spatial resolution. Past climatic variables were downloaded from PaleoClim (Brown et al. 2018). These variables include climatic data for the Pliocene M2 (3.3 Ma), Pleistocene Last Interglacial (130 ka), and Pleistocene Last Glacial Maximum (21 ka)

downloaded at 2.5 min resolution (Dolan et al. 2015; Otto-Bliesner et al. 2006; Karger et al. 2021). Future bioclimatic variables for 2081-2100 were downloaded from WorldClim at 2.5 min resolution from the EC-Earth-Veg global climate model (GCM) for Shared Socioeconomic Pathway (SSP) 3-7.0 (EC-Earth Consortium 2019). All nineteen bioclimatic variables were selected for creating the modern, Last Interglacial, Last Glacial Maximum, and 2081-2100 models. The fourteen available bioclimatic variables for the Pliocene M2 were selected for the model.

North America ecoregion data were downloaded from the Environmental Protection Agency (EPA) (https://www.epa.gov/eco-research/ecoregions-north-america). Ecoregion III was selected for its high resolution of regional division across the continent.

Analyses

Models were developed using Maximum Entropy Modeling (MaxEnt). Each map used a bias file to correct any sampling biases by reducing the sampling area to within 0.5 decimal degrees (or ~55.6 km) of rarefied *Castor canadensis* occurrence points. The bias file was created using the Gaussian Kernel Density of sampling localities tool on SDM toolbox in ArcGIS.

Instead of splitting point data into testing (20%) and training (80%) points, all point data were replicated using bootstrapping. This allowed MaxEnt to repeatedly run through sampling without the need for prior data separation and eliminated any potential bias associated with data sub-setting.

Modern distribution maps of *C. canadensis* were produced to determine a baseline for current habitat suitability across North America. Three maps were produced: one using strictly

bioclimatic variables, one using strictly EPA Level III ecoregions, and one using both bioclimatic variables and EPA Level III ecoregions.

Three past projection models for the mid-Pliocene, Last Interglacial, and Last Glacial Maximum, and one future projection for 2081-2100 were produced. Models for each time bin show predicted species suitability across North America in addition to changes in habitat suitability compared to modern bioclimatic data. Fossil occurrences for *Castor* were overlaid to compare model accuracy to known localities.

CHAPTER 3. RESULTS

Geometric Morphometrics

Relative Warp Analysis

Relative warp analyses were run for each view of the cranium and dentary. Significant warps were determined for each view by Eigenvalues produced from the analysis. Warps with Eigenvalues greater than one were deemed significant to shape variation.

The relative warp scores for the dorsal view produced seven significant warps, explaining 81.5% of the observed shape variation. Relative warps 1 and 2 showed separation of *Castor fiber* from overlapping *C. canadensis* and *C. californicus*, as shown in Figure 6. Dorsal relative warp 1 (DRW1) explained 27.64% of the variation, with *C. fiber* clustered with negative scores while *C. californicus* clustered with positive scores. *C. canadensis* clustered near zero, spanning both positive and negative values. Positive DRW1 scores are associated with shortened nasals, wider posterior cranium, and posterior positioning of orbit (Figure 7). Negative DRW1 scores are associated with elongated nasals, constricted posterior cranium, and anterior positioning of the orbit. DRW2 explained 17.03% of the variation, with *C. fiber* and *C. californicus* both tended towards positive scores, while *C. canadensis* remained widespread in both positive and negative scores. Positive DRW2 scores are associated with shortened rostrum, constriction of posterior cranium, and widened zygomatic arches (Figure 7). Negative DRW2 scores are associated with elongated rostrum, widening of posterior cranium, and narrow zygomatic arches.

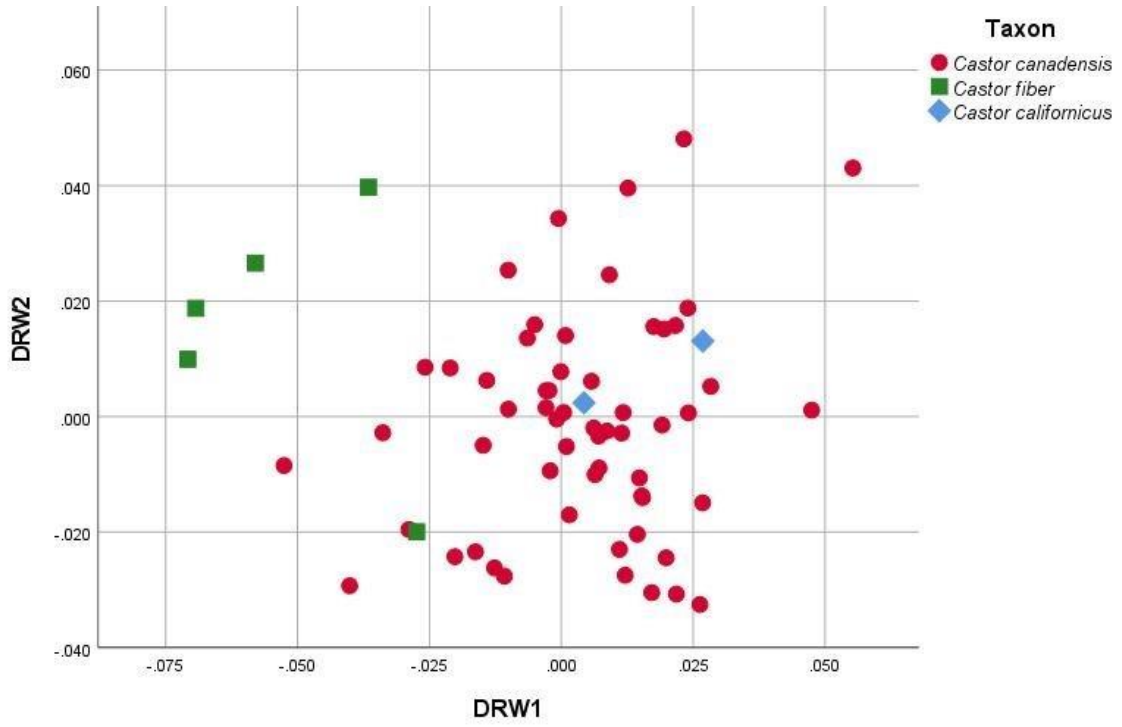

Figure 6. Relative warp plot for the dorsal view of the cranium. Axes depict shape variation, associated with landmark deformations depicted in Figure 7

Relative Warp	Deformation (-)	Deformation (+)
DRW1	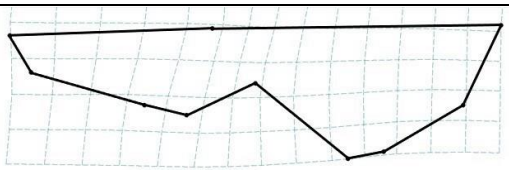	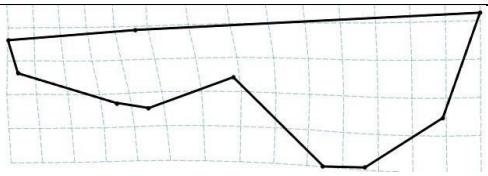
DRW2	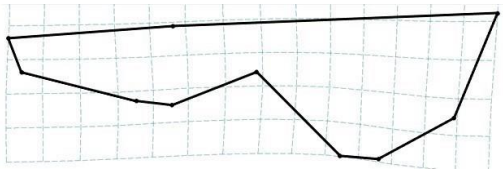	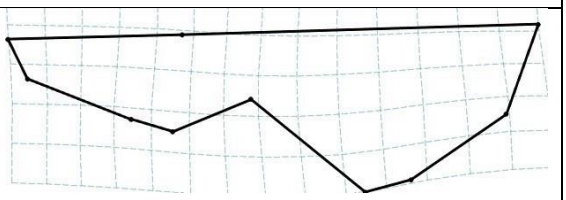
LRW1	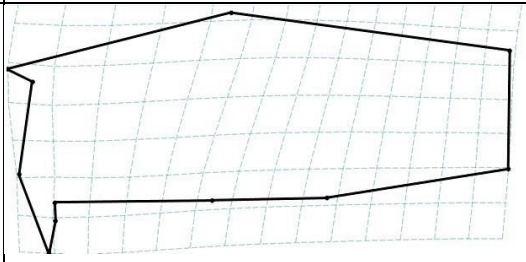	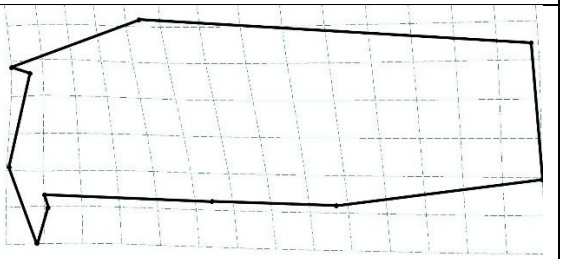
LRW3	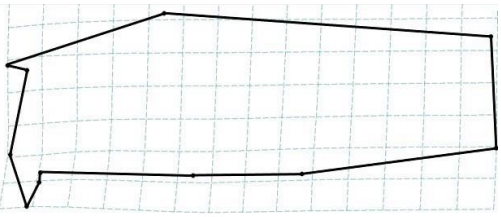	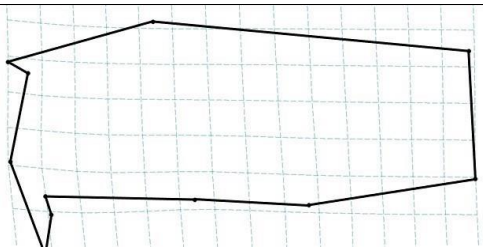

Figure 7. Thin plate splines indicate landmark deformation for the dorsal, lateral, and ventral views of the cranium

Relative warp scores for the lateral view produced eight significant warps, explaining 92.73% of the observed shape variation. Relative warps 1 and 3 showed good separation of *C. fiber* and *C. canadensis*, as shown in Figure 8. Lateral relative warp 1 (LRW1) explained 45.97% of the variation, with *Castor fiber* associated with negative scores, *C. californicus* with near zero to negative scores, and *C. canadensis* spread over both positive and negative scores. Negative LRW1 scores associated with elongated nasals and shortened posterior cranium between nuchal crest and occipital condyles (Figure 7). Positive LRW1 scores are associated with shortened

nasals and widened posterior cranium near occipital condyles. LRW3 explained 16.57% of the variation, with *C. fiber* clustered with negative scores while *C. canadensis* and *C. californicus* showed widespread distributions across positive and negative scores. Negative LRW3 scores associated with more anteroventral position of nasals and narrowing posterior cranium between nuchal crest and occipital condyles (Figure 7). Positive RW3 scores associated with posterior position of nasals and widening posterior cranium between nuchal crest and occipital condyles.

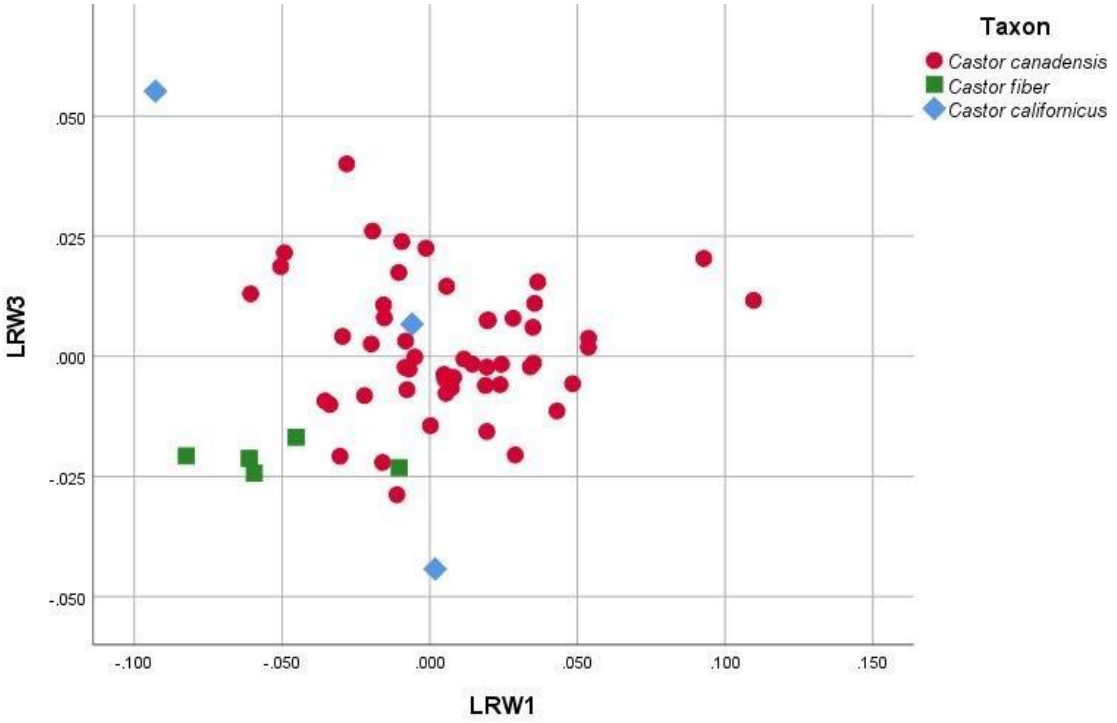

Figure 8. Relative warp plot for the lateral view of the cranium. Axes depict shape variation, associated with landmark deformations depicted in Figure 7

The relative warp scores for the ventral view produced six significant warps, explaining 83.52% of the observed shape variation (Table 4). None of the six relative warps showed clear separation of species.

Table 4. Significant relative warps (Eigenvalues>1) and variance percentage attributed to shape deformation for ventral relative warps

Relative Warp	Variance
1	29.03%
2	20.25%
3	11.08%
4	9.36%
5	7.58%
6	6.21%

The relative warp scores for the dentary produced eleven significant warps, explaining 92.87% of the observed shape variation. Relative warps 1 and 2 showed significant separation between groups, as shown in Figure 9. Dentary relative warp 1 (DenRW1) explained 27.71% of the variation, with *Castor fiber* clustering in positive scores, *C. californicus* in negative and near 0 positive scores, and *C. canadensis* spanning both positive and negative scores. Negative DenRW1 scores are associated with posterior placement of anterior margin of pterygoid insertion and posterior widening from the coronoid process to the angular process (Figure 9). Positive DenRW1 scores are associated with anterior placement of anterior margin of pterygoid insertion and posterior narrowing of the coronoid process to the angular process. DenRW2 explained 14.62% of the variation, with *C. fiber* grouping with negative scores, *C. californicus* with positive scores, and *C. canadensis* with both negative and positive scores clustering around zero. Positive DenRW2 scores are associated with widening area between articular surface of mandibular condyle and curve between the condylar and angular process, posterior widening from the coronoid process to the angular process, and dorsal migration of anteroventral boarder or incisive alveolus (Figure 9). Negative DenRW2 scores are associated with narrowing area between articular surface of mandibular condyle and curve between the condylar and angular

process, posterior constriction between the coronoid process to the angular process, and ventral migration of anteroventral boarder or incisive alveolus.

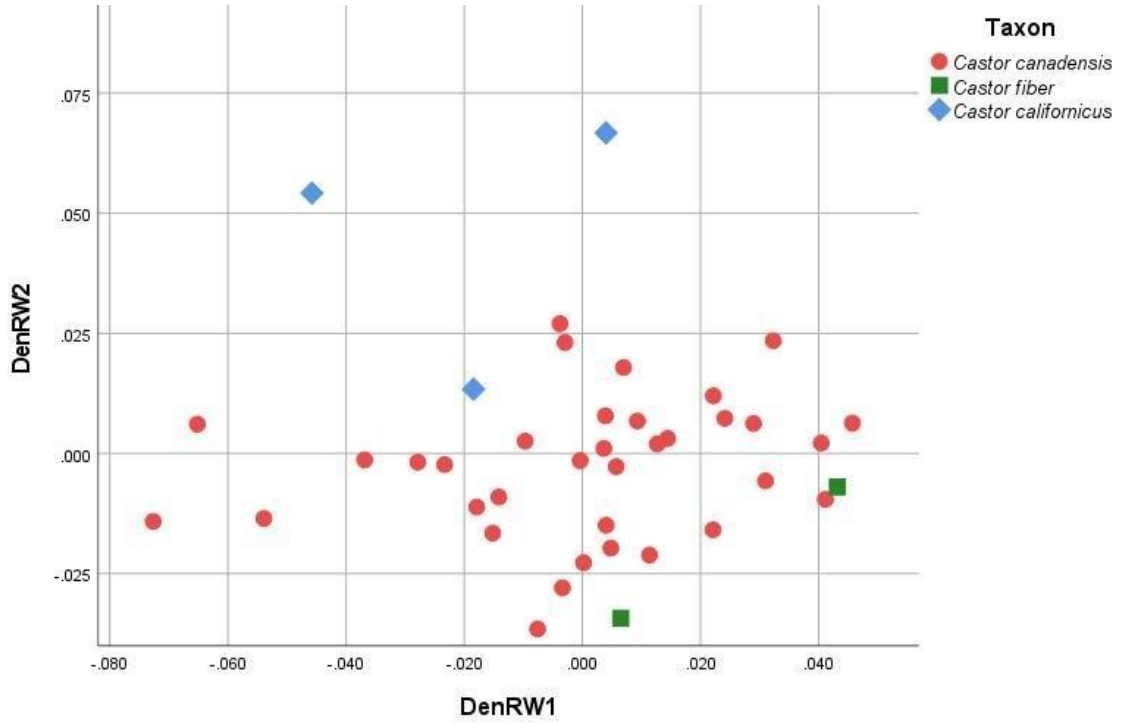

Figure 9. Relative warp plot for the dentary. Axes depict shape variation, associated with landmark deformations depicted in Figure 10

Relative Warp	Deformation (-)	Deformation (+)
DenRW1	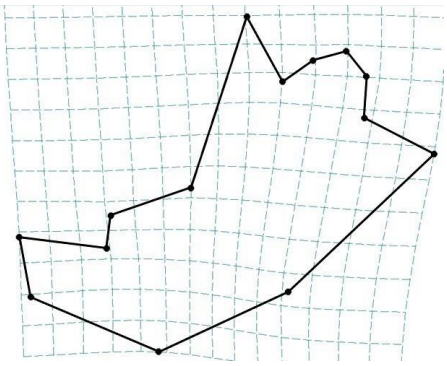	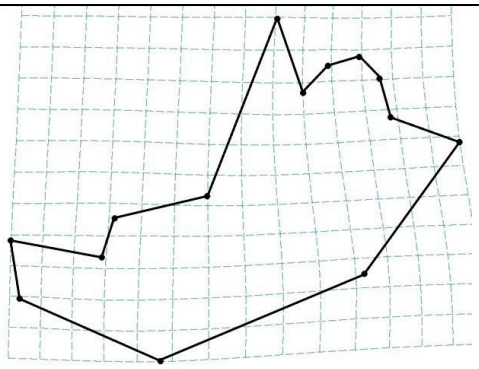
DenRW2	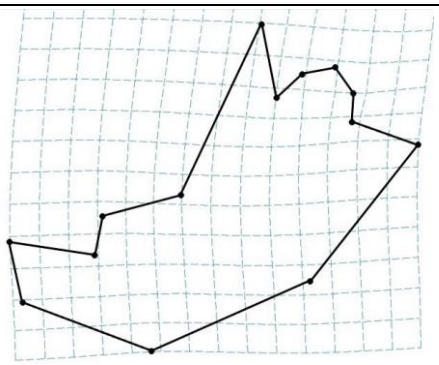	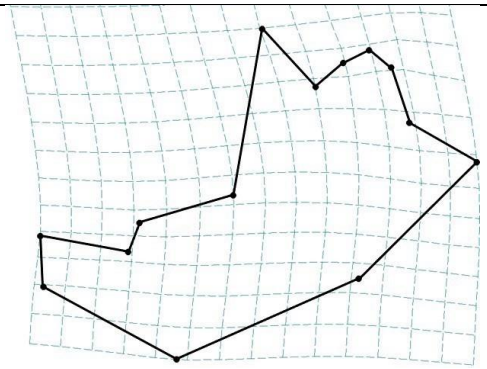

Figure 10. Thin plate splines indicate the amount of deformation for the dentary

Castor fiber and *C. canadensis* showed minimal overlap within the relative warp analysis. *C. californicus* plotted either within or near the range of *C. canadensis* and consistently fell outside of the plotted range for *C. fiber*.

Stepwise Canonical Variate Analysis

Cranial and dentary data were analyzed separately within the two subsequent CVAs. The first CVA used both *Castor canadensis* and *C. fiber* as *a priori* categories with *C. californicus* classified as unknown (Tables 5 and 7). The second CVA categorized all three species individually into *a priori* categories (Tables 6 and 8).

The first cranial stepwise model, with *Castor californicus* categorized as unknown, included 9 of the 21 partial warps and showed good separation of groups (Wilk's lambda = 0.173, $F_{(1,56)} = 24.360$, $p < 0.00$). The analysis yielded one canonical variate which accounted for 100% of the variance in the dataset. A histogram of CV scores is shown in Figure 11.

Canonical variate 1 (CV1) accounted for 100% of the variance and showed separation of *Castor fiber* with high negative scores, *C. californicus* with lower negative scores, and *C. canadensis* with both positive and negative scores distributed around 0. Positive CV1 scores are associated with shortened nasals, posteromedial position of the orbit, and widening of the posterior cranium (Figure 12).

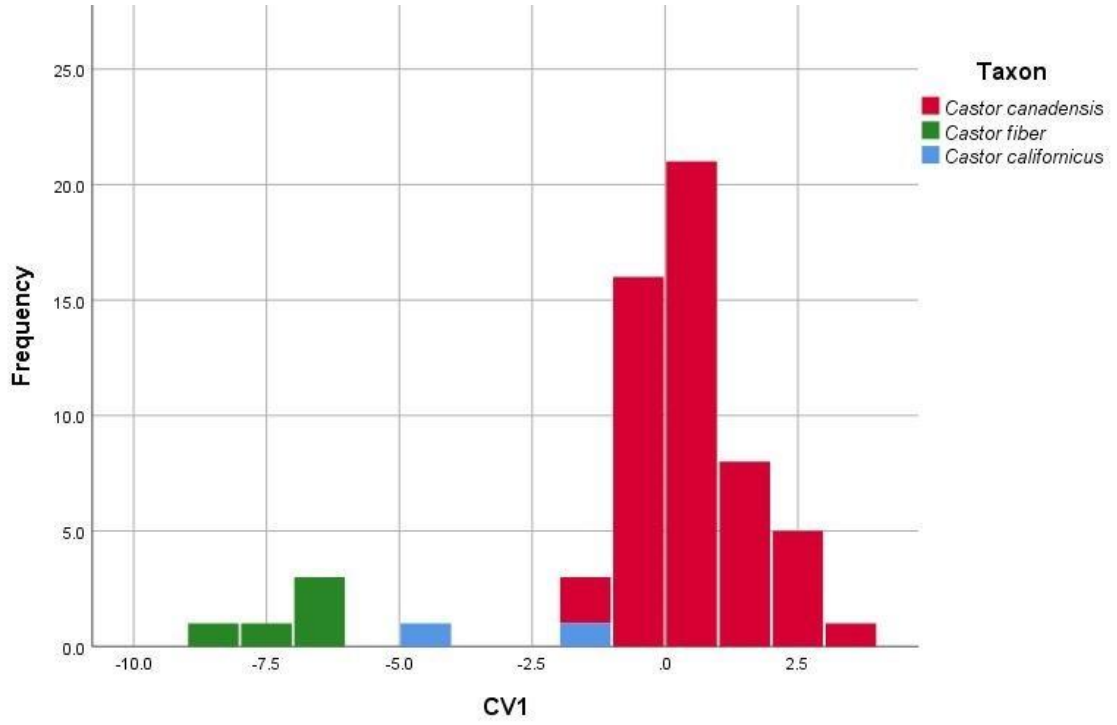

Figure 11. Histogram of canonical variate for analysis of cranial data. Axis depicts changes in shape, associated with shape deformations referenced in Figure 12

Table 5. Summary statistics for cranial Canonical Variate Analysis with *Castor californicus* uncategorized

	CV1
Eigenvalue	4.766
% Variance Explained	100
Wilk's Lambda	0.173
Chi Squared (X^2)	86.724
Canonical Correlation	0.909

	Deformation (-)	Deformation (+)
CV1	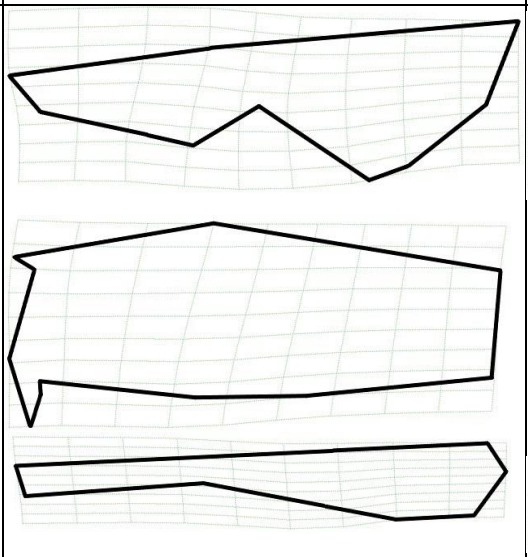	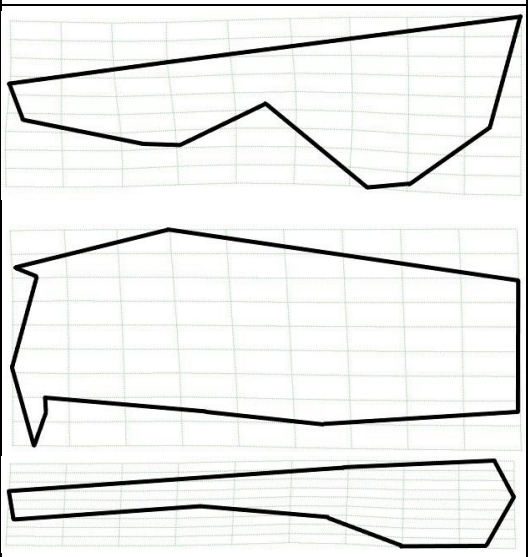

Figure 12. Thin plate splines indicate the amount of deformation associated with the canonical variate axis for the dorsal, lateral, and ventral views of the cranium

The second cranial stepwise model, with all specimens categorized *a priori*, included 11 of the 21 partial warps and showed significant separation of groups (Wilk's lambda 0.056, $F_{(1,56)}$ = 13.198, $p < 0.00$). This analysis yielded two canonical variates, which accounted for 100% of the variance in the dataset. A scatterplot of group classification is shown in Figure 13.

CV1 accounted for 63.5% of the variance and showed good separation of taxa (Figure 13), *Castor fiber* and *C. californicus* both had positive scores, while *C. canadensis* clustered around 0, with both positive and negative scores. Negative CV1 scores associated with shortened nasals, widening posterior cranium, and widening premaxilla (Figure 13).

CV2 accounted for 36.5% of the variance and additionally showed good separation of species (Figure 14), *Castor fiber* had negative scores, *C. californicus* had highly positive scores,

and *C. canadensis* had scores close to 0, with some in both positive and negative scores. Positive CV2 scores associated with shortened nasals and broader posterior cranium (Figure 13).

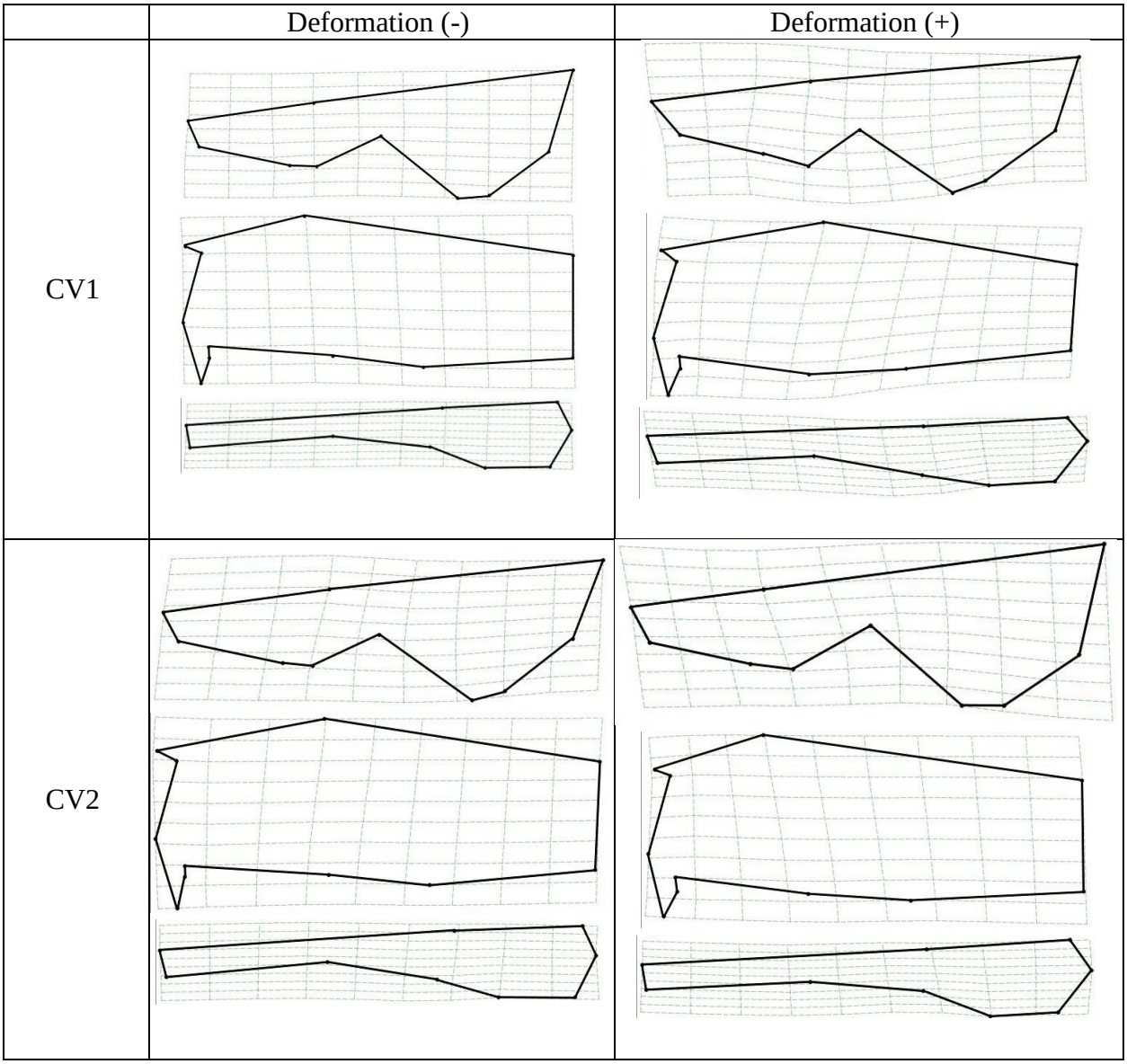

Figure 13. Thin plate splines indicate the amount of deformation associated with each canonical variate axis for the dorsal, lateral, and ventral views of the cranium

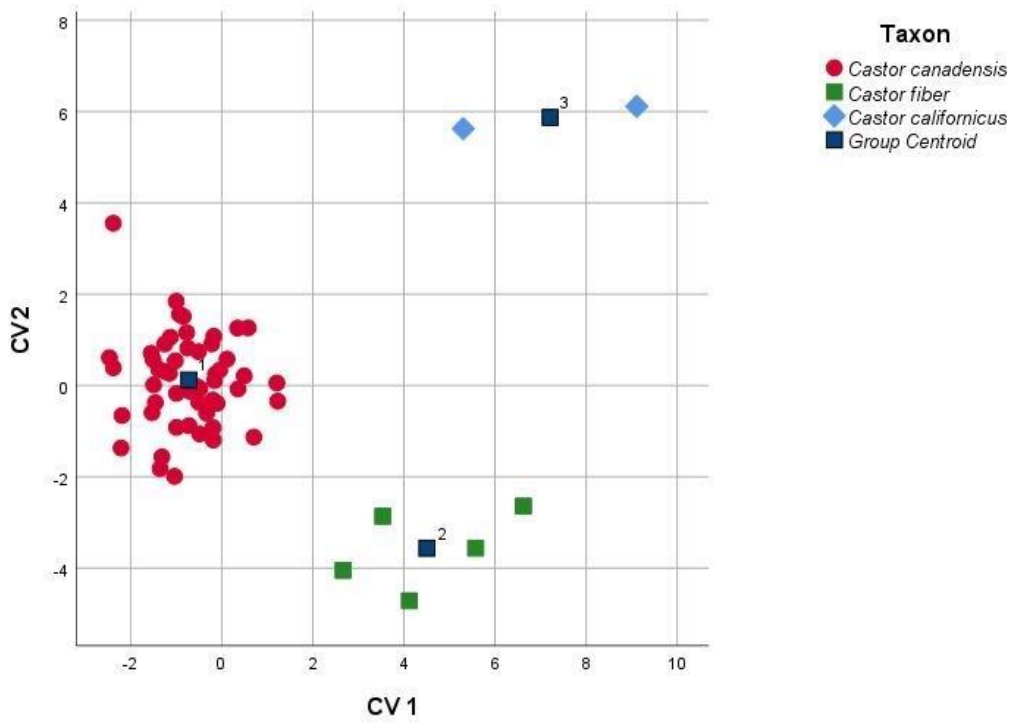

Figure 14. Canonical variate plot for analysis of cranial data. Axes depict changes in shape, associated with shape deformations referenced in Figure 13

Table 6. Summary statistics for cranial Canonical Variate Analysis with all species categorized *a priori*

	CV1	CV2
Eigenvalue	4.221	2.421
% Variance Explained	63.5	36.5
Wilk's Lambda	0.056	0.292
Chi Squared (X^2)	144.131	61.501
Canonical Correlation	.899	.841

The dentary stepwise model, which initially had *Castor californicus* categorized as unknowns, included 6 of the 11 partial warps and showed some separation of groups (Wilk's lambda = 0.351, $F_{(1, 40)} = 9.246$, $p < 0.00$). The analysis yielded one canonical variate which

accounted for 100% of the variance in the dataset. A histogram of group classification is shown in Figure 15.

CV1 accounted for 100% of the variance and showed good separation of groups (Figure 14), *Castor fiber* had high positive scores, *C. californicus* overlapped with *C. canadensis*, but only as negative and near 0 scores, and *C. canadensis* centered just negative of zero and contained positive and negative scores. Negative CV1 scores associated with anterior positioning of anterior margin of angular process, dorsal movement of curvature between coronoid and condylar processes, and anteroventral movement of coronoid process (Figure 16).

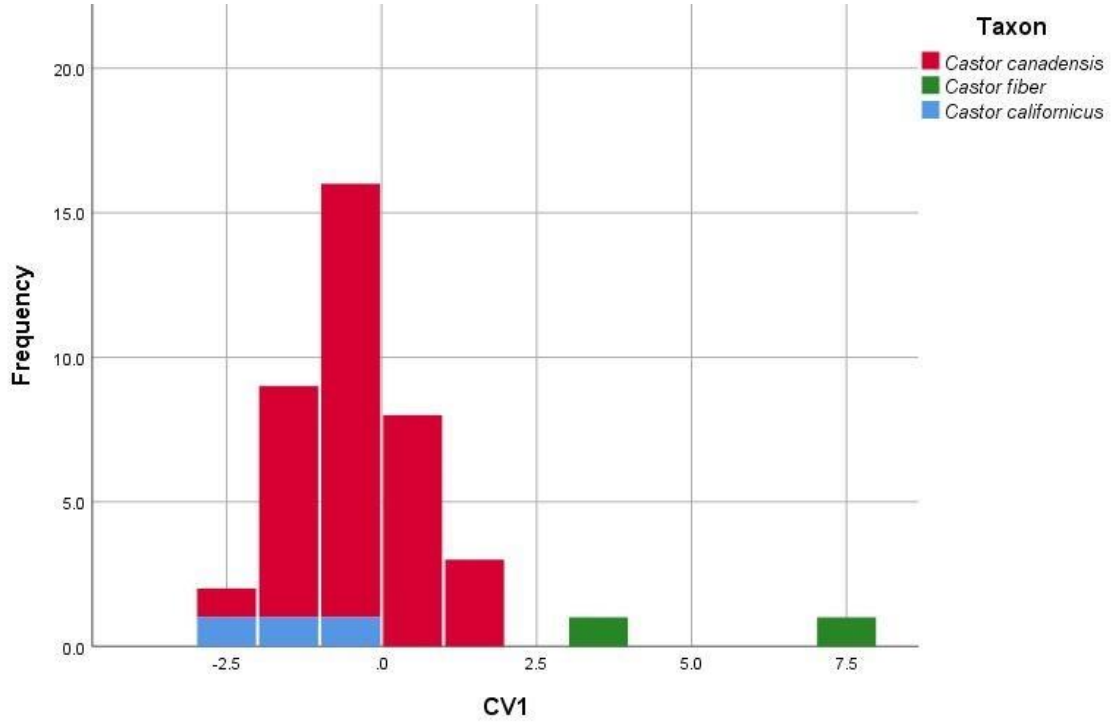

Figure 15. Histogram of canonical variate for analysis of dentary data. Axis depicts changes in shape, associated with shape deformations referenced in Figure 16

Table 7. Summary statistics for dentary Canonical Variate Analysis with *Castor californicus* uncategorized

	CV1
Eigenvalue	1.849
% Variance Explained	100
Wilk's Lambda	0.351
Chi Squared (X^2)	33.504
Canonical Correlation	0.806

	Deformation (-)	Deformation (+)
CV1	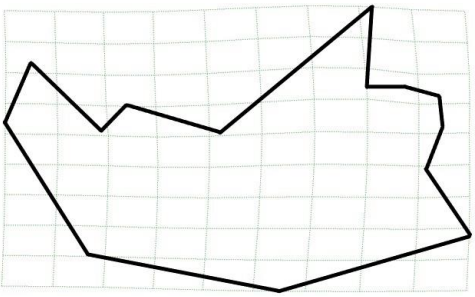	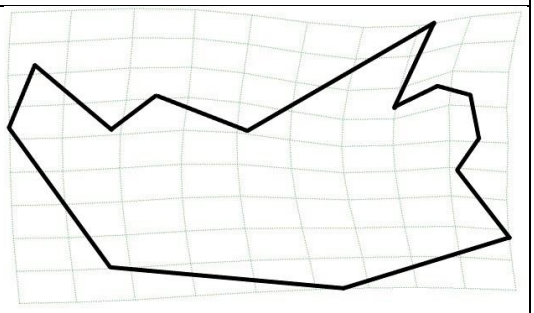

Figure 16. Thin plate splines indicate the amount of deformation associated with the canonical variate axis for the dentaries

The second dentary stepwise model, with all species categorized *a priori*, included 3 of the 11 partial warps and showed significant separation of groups (Wilk's lambda = 0.329, $F_{(2,40)}$ = 8.658, $p < 0.00$). This analysis yielded two canonical variates, which accounted for 100% of the variance in the dataset. A scatterplot of group classification is shown in Figure 18.

CV1 accounted for 80.5% of the variance and showed separation of (Figure 18) *Castor californicus* with negative scores from *C. fiber* with positive scores, and *C. canadensis* with

scores centered around 0, but some spread into positive and negative scores. Positive CV1 scores associated with posterior positioning of coronoid process, shortening of condylar process, dorsal positioning of angular process, and shortened tooth row (Figure 17).

CV2 accounted for 19.5% of the variance and showed some separation of groups (Figure 18), *C. californicus* had positive scores and near 0 values, *C. fiber* had highly positive values, and *C. canadensis* clustered near 0 in both positive and negative scores. Positive CV2 scores associated with posterior positioning of the horizontal ramus, ventral positioning of angular process, and anterior positioning of coronoid process (Figure 17).

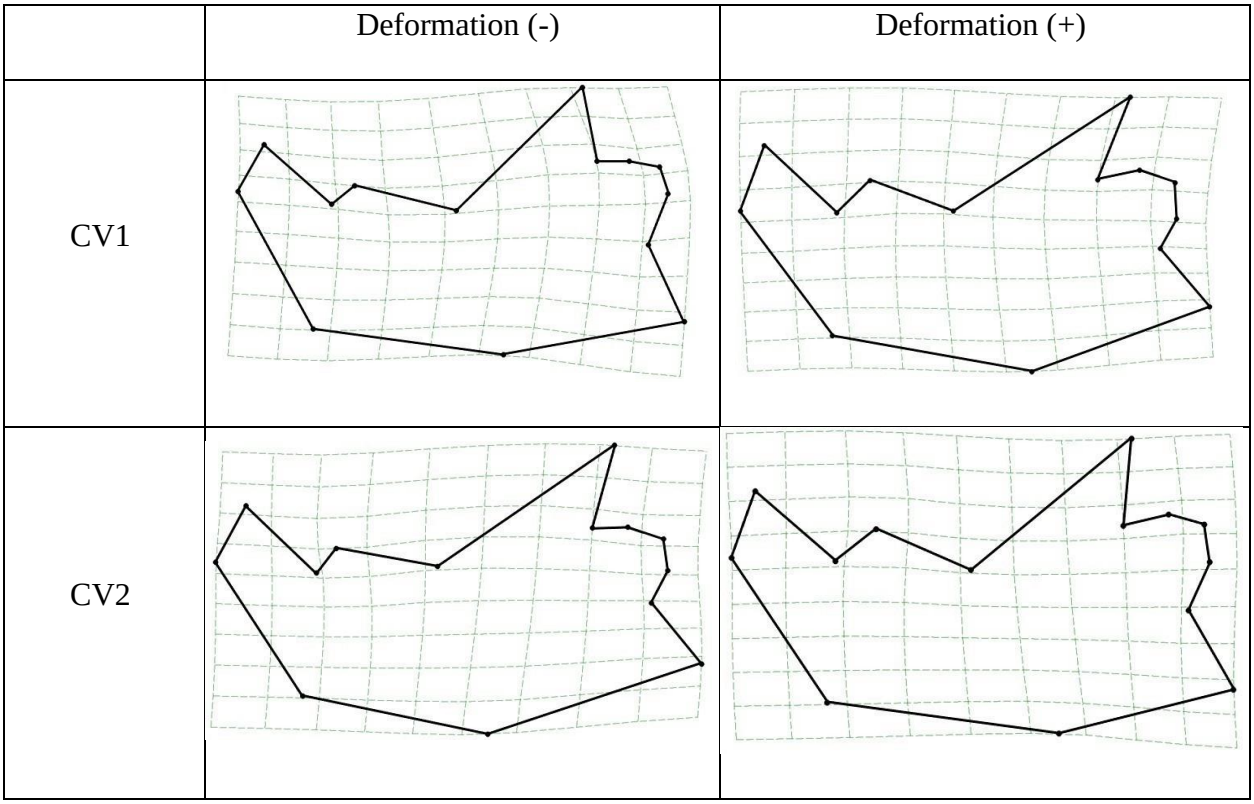

Figure 17. Thin plate splines indicate the amount of deformation associated with each canonical variate axis for the dentaries

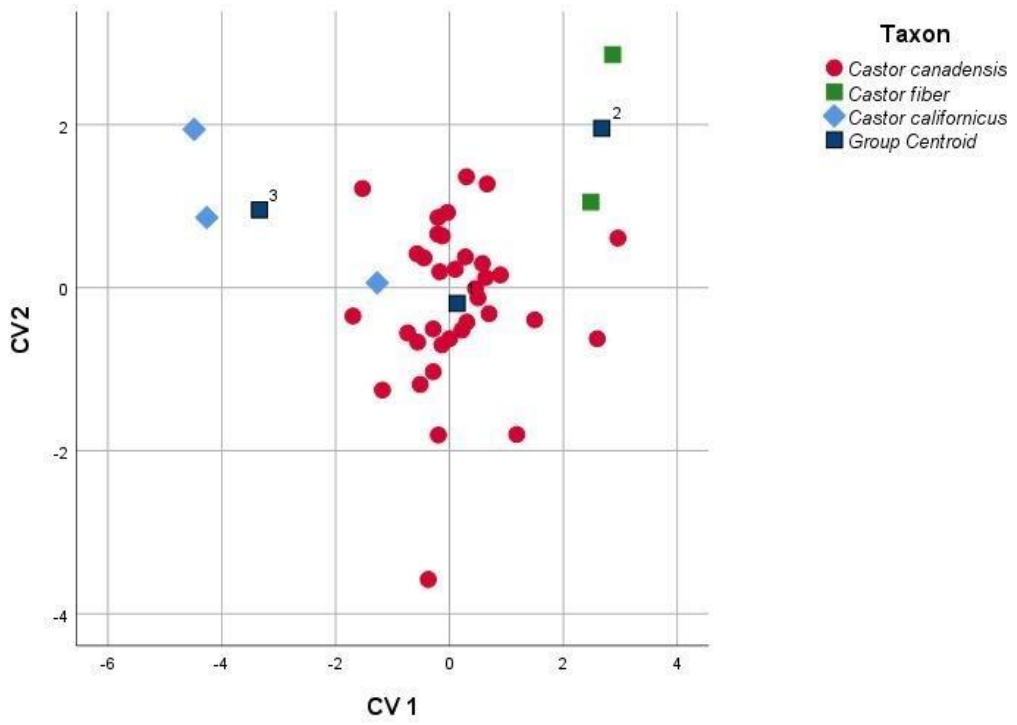

Figure 18. Canonical variate plot for analysis of dentary data. Axes depict changes in shape, associated with shape deformations referenced in Figure 17

Table 8. Summary statistics for dentary Canonical Variate Analysis with all species categorized *a priori*

	CV1	CV2
Eigenvalue	1.307	0.316
% Variance Explained	80.5	19.5
Wilk's Lambda	0.329	0.760
Chi Squared (X^2)	39.968	9.876
Canonical Correlation	0.753	0.490

The classification stage of the CVA was used to determine the accuracy for individual specimens to be separated into species. Classification occurred in two steps: group classifications

and cross-validation, where specimens were excluded from the model and reevaluated using the remaining specimens in the analysis.

The first cranial CVA classification resulted in 100% correct classification of individuals with 98.3% correct classification when cross-validated. One specimen of *Castor canadensis* was classified as *C. fiber* in cross-validation. *C. californicus*, which was assigned as unknown for this cranial CVA, were classified as both *C. fiber* and *C. californicus*. Those specimens assigned to alternate species classifications produced low conditional probabilities, which would suggest incorrect classifications of those specimens during analysis. Classifications and percentages of specimen classifications into species are shown in Table 9.

Table 9. Results of cranial CVA classification with *Castor californicus* assigned as unknown

		Taxon	*Castor canadensis*	*Castor fiber*	Total
Original	Count	*C. canadensis*	53	0	53
		C. fiber	0	5	5
		C. californicus	1	1	2
	%	*C. canadensis*	100	0	100
		C. fiber	0	100	0
		C. californicus	50	50	100
Cross-validated	Count	*C. canadensis*	52	1	53
		C. fiber	0	5	5
	%	*C. canadensis*	98.1	1.9	100
		C. fiber	0	100	100

The second cranial CVA classification, in which all species were assigned *a priori*, resulted in 100% correct classification of individuals with 98.3% correct classification when cross validated. One specimen of *C. californicus* was categorized as *C. canadensis* in cross-validation. The specimen produced low conditional probabilities, which would suggest incorrect

classification of that specimen into *C. canadensis*. Classifications and percentages of specimen classifications into species are shown in Table 10.

Table 10. Results of cranial CVA classification with all species assigned *a priori*

		Taxon	*Castor canadensis*	*Castor fiber*	*Castor californicus*	Total
Original	Count	*C. canadensis*	51	0	0	51
		C. fiber	0	5	0	5
		C. californicus	0	0	2	2
	%	*C. canadensis*	100	0	0	100
		C. fiber	0	100	0	100
		C. californicus	0	0	100	100
Cross-validated	Count	*C. canadensis*	51	0	0	51
		C. fiber	0	5	0	5
		C. californicus	1	0	1	2
	%	*C. canadensis*	100	0	0	100
		C. fiber	0	100	0	100
		C. californicus	50	0	50	100

Dentary CVA classification, where *Castor californicus* was assigned as unknown, resulted in 100% correct classification of individuals with 97.3% correct classification when cross-validated. *C. californicus* was categorized as both *C. canadensis* and *C. fiber* in cross-validation. Conditional probabilities for those specimens fall within the range of variation for both *C. canadensis* and *C. fiber*, suggesting more confidence in resulting assigned species classifications. Classifications and percentages of specimen classifications into species are shown in Table 11.

Table 11. Results of dentary CVA classification with *Castor californicus* assigned as unknown

		Taxon	*Castor canadensis*	*Castor fiber*	Total
Original	Count	*C. canadensis*	35	0	35
		C. fiber	0	2	2
		C. californicus	3	0	3
	%	*C. canadensis*	100	0	100
		C. fiber	0	100	100
		C. californicus	100	0	100
Cross-validated	Count	*C. canadensis*	35	0	35
		C. fiber	1	1	2
	%	*C. canadensis*	100	0	100
		C. fiber	50	50	100

Dentary CVA classification in which all species were assigned a priori resulted in 95% correct classification of individuals with 92.5% correct classification when cross-validated. In this analysis, some specimens were misclassified between groups. One specimen of *Castor canadensis* was classified as *C. fiber* in both the original classification and cross validation. One specimen of *C. fiber* was classified as *C. canadensis* in cross validation and one specimen of *C. californicus* was classified as *C. canadensis*. Conditional probabilities for those specimens fall within the range of variation for each species, suggesting more confidence in resulting assigned species classifications. Classifications and percentages of specimen classifications into species are shown in Table 12.

Table 12. Results of dentary CVA classification with all species assigned *a priori*

		Taxon	*Castor canadensis*	*Castor fiber*	*Castor californicus*	Total
Original	Count	*C. canadensis*	34	1	0	35
		C. fiber	0	2	0	2
		C. californicus	1	0	2	3
	%	*C. canadensis*	97.1	2.9	0	100
		C. fiber	0	100	0	100
		C. californicus	33.3	0	66.7	100
Cross-validated	Count	*C. canadensis*	34	1	0	35
		C. fiber	1	1	0	2
		C. californicus	1	0	2	3
	%	*C. canadensis*	97.1	2.9	0	100
		C. fiber	50	50	0	100
		C. californicus	33.3	0	66.7	100

Cluster Analysis

Hierarchical cluster analysis was conducted using uniform components and partial warp scores to examine how specimens grouped together without *a priori* categorization of species. Two separate analyses were conducted with cranial and dentary data.

Cranial cluster analysis, shown in Figure 19, resulted in some separation between species. All specimens of *Castor fiber* grouped together, except for one specimen (MVZ 19229), which clustered with *C. canadensis*. This specimen consistently clustered separately from the other *C. fiber* specimens, as shown in the relative warp graphs produced from the RWA. This separation could be attributed to MVZ 19229 having more distinct morphological differences compared to the other *C. fiber* specimens included in the analysis, including an elongated rostrum, narrow zygomatic arches, and widened posterior cranium.

Castor canadensis specimens grouped together, with *C. californicus* fitting into the *C. canadensis* cluster. An outgroup, formed by three specimens, formed outside of the *C. canadensis* and *C. fiber* clusters. Those specimens included two *C. canadensis* (MVZ 80744 and UCLA 9517) and one *C. californicus* (USNM 26154). Uniform components and partial warp scores of those three outlier specimens showed no clear indication of similarities or extreme variation in scores which might separate those specimens from the other *C. canadensis* group.

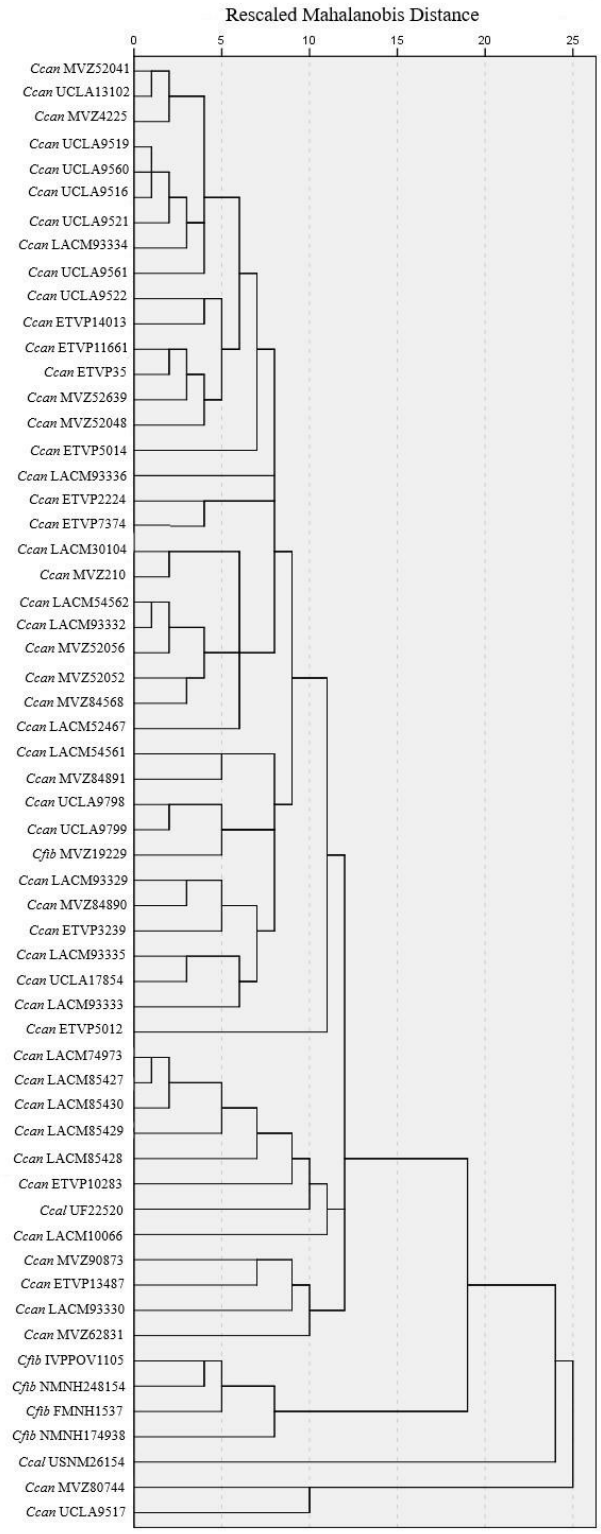

Figure 19. Dendrogram of cranial cluster analysis. Specimens used in analysis are labeled by species and catalog number

Dentary cluster analysis, shown in Figure 20, resulted in two prominent groupings. All *Castor canadensis* grouped together, with *C. fiber* specimens (USNM 174938 and USNM 248154) grouped within *C. canadensis* specimens. *C. californicus* (and *C. accessor*) clustered together, forming the outgroup from *C. canadensis*.

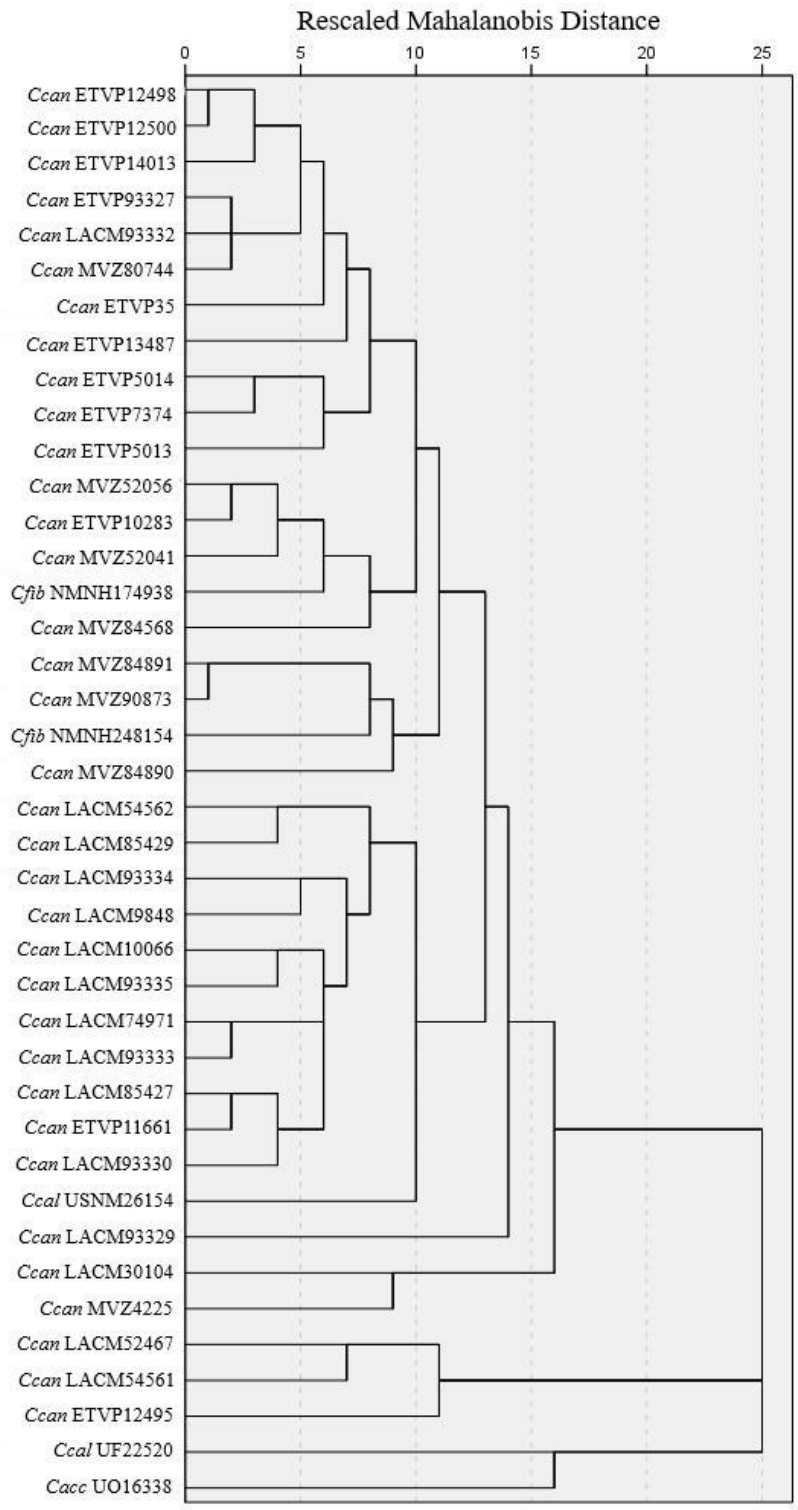

Figure 20. Dendrogram of dentary cluster analysis. Specimens used in analysis are labeled by species and catalog number

Postcranial Analysis

Descriptive Statistics and ANOVA

Descriptive statistics for postcranial measurements, including mean values, standard deviations, minimum and maximum values, were calculated for each species (Table 13). Univariate ANOVAs showed significant differences between species across postcrania, as shown with descriptive statistics in Table 13.

Castor californicus had significantly larger mean values than *C. canadensis* for most variables in this analysis. Range values, determined by maximum and minimum measurements, showed that *C. californicus* had substantial overlap in ranges when compared to those of *C. canadensis*. *C. fiber* resulted in limited mean and range values due to inadequate sampling.

Postcranial elements with little overlap in range values include FeAPD and TDEMLD (Table 13, Figure 21). *Castor californicus* had a broad femur anteroposterior diameter (FeAPD) compared to *C. canadensis*. *C. californicus* also has a wider mediolateral diameter on the distal end of the tibia (TDEMLD) than *C. canadensis*.

Elements which had no overlap in range values between *C. californicus* and *C. canadensis* include HDAW, FeEB, TDEAPD, MT3APD, and MT4MLD (Table 13, Figure 22). *C. californicus* has a wider humeral articular width at the distal end (HDAW), anteroposterior diameter of the 3rd metatarsal (MT3APD), and mediolateral diameter of the 4th metatarsal (MT4MLD) than *C. canadensis*. *C. californicus* also has a broader anteroposterior distal end of the tibia (TDEAPD) and femoral epicondylar breadth (FeEB) than *C. canadensis.*

Table 13. Descriptive statistics, coefficients of variation, and ANOVA results for species postcranial measurements. Statistically significant *p*-values bolded for clarity

Measurement	Taxon	N	Mean (μ)	St. Dev (σ)	Min	Max	CoVar (%)	F (df)	*p*
HMLD	*C. canadensis*	22	10.75	0.76	9.55	12.00	7.10	14.20 (2)	***0.00***
	C. fiber	1	7.49		7.49	7.49			
	C. californicus	3	12.31	1.06	11.27	13.38	8.57		
HDAW	*C. canadensis*	21	19.85	0.80	18.18	21.22	4.03	26.85 (1)	***0.00***
	C. fiber	0	-	-	-	-	-		
	C. californicus	4	22.01	0.44	21.64	22.62	1.99		
UL	*C. canadensis*	20	119.66	4.01	112.99	130.28	3.35	29.57 (2)	***0.00***
	C. fiber	1	85.07	-	85.07	85.07	-		
	C. californicus	3	124.47	8.32	115.01	130.64	6.68		
ULOL	*C. canadensis*	20	25.23	1.68	22.28	28.57	6.66	14.80 (2)	***0.00***
	C. fiber	1	16.29	-	16.29	16.29	-		
	C. californicus	3	23.91	0.98	23.30	25.04	4.10		
FeL	*C. canadensis*	24	99.75	5.59	89.44	110.81	5.60	20.80 (2)	***0.00***
	C. fiber	2	77.93	12.52	69.08	86.78	16.06		
	C. californicus	6	109.82	6.45	98.70	117.27	5.87		
FeAPD	*C. canadensis*	24	11.78	1.03	9.93	13.40	8.73	12.33 (3)	***0.00***
	C. fiber	2	10.60	2.49	8.84	12.36	23.48		
	C. californicus	8	14.08	0.86	13.21	15.60	6.09		
FeMLD	*C. canadensis*	24	24.94	1.52	21.18	27.94	6.08	2.69 (3)	0.06
	C. fiber	2	21.78	7.75	16.30	27.26	35.58		
	C. californicus	9	26.56	2.55	23.13	31.05	9.62		
FeGT	*C. canadensis*	23	13.17	1.99	10.27	18.07	15.08	4.07 (1)	0.05
	C. fiber	0	-	-	-	-	-		
	C. californicus	6	15.29	3.31	11.98	19.36	21.65		
FeHD	*C. canadensis*	21	17.16	0.65	16.10	19.22	3.82	64.66 (1)	***0.00***
	C. fiber	0	-	-	-	-	-		
	C. californicus	6	20.20	1.27	18.15	21.55	6.27		
FeEB	*C. canadensis*	22	34.13	1.81	30.44	37.10	5.32	58.22 (1)	***0.00***
	C. fiber	0	-	-	-	-	-		
	C. californicus	5	41.72	2.81	39.79	46.57	6.74		
TL	*C. canadensis*	19	131.29	5.23	119.75	142.91	3.99	12.81 (1)	***0.00***
	C. fiber	0	-	-	-	-	-		
	C. californicus	3	145.75	13.28	131.08	156.97	9.11		

TAPD	*C. canadensis*	19	14.64	1.62	11.02	17.03	11.05	0.76 (1)	0.39
	C. fiber	0	-	-	-	-	-		
	C. californicus	4	13.89	1.19	12.40	15.24	8.59		
TMLD	*C. canadensis*	19	12.97	1.20	10.74	15.67	9.29	8.38 (1)	***0.01***
	C. fiber	0	-	-	-	-	-		
	C. californicus	4	15.12	2.00	13.28	17.41	13.22		
TPEMLD	*C. canadensis*	18	32.61	1.24	30.94	35.50	3.80	12.26 (1)	***0.00***
	C. fiber	0	-	-	-	-	-		
	C. californicus	3	36.23	3.61	32.14	38.99	9.97		
TDEAPD	*C. canadensis*	18	16.34	0.75	15.17	17.78	4.59	27.86 (1)	***0.00***
	C. fiber	0	-	-	-	-	-		
	C. californicus	4	18.38	0.23	18.20	18.69	1.25		
TDEMLD	*C. canadensis*	18	19.08	1.03	16.92	20.67	5.38	21.20 (1)	***0.00***
	C. fiber	0	-	-	-	-	-		
	C. californicus	5	21.88	1.78	20.17	24.53	8.11		
TLOF	*C. canadensis*	18	39.98	3.56	33.94	45.48	8.90	1.10 (1)	0.31
	C. fiber	0	-	-	-	-	-		
	C. californicus	3	37.56	4.81	33.18	42.71	12.81		
MT3L	*C. canadensis*	16	49.04	3.46	45.35	59.76	7.05	3.58 (1)	0.08
	C. fiber	0	-	-	-	-	-		
	C. californicus	3	53.22	3.88	49.03	56.70	7.30		
MT3APD	*C. canadensis*	8	6.20	0.34	5.66	6.71	5.48	25.61 (1)	***0.00***
	C. fiber	0	-	-	-	-	-		
	C. californicus	5	7.90	0.87	7.09	9.35	11.01		
MT3MLD	*C. canadensis*	8	7.58	0.53	6.65	8.16	6.98	10.31 (1)	***0.00***
	C. fiber	0	-	-	-	-	-		
	C. californicus	5	9.06	1.15	7.25	9.95	12.66		
MT4L	*C. canadensis*	13	56.73	2.23	52.76	60.78	3.93	12.03 (1)	***0.00***
	C. fiber	0	-	-	-	-	-		
	C. californicus	4	61.22	2.39	58.08	63.52	3.90		
MT4APD	*C. canadensis*	6	7.59	0.18	7.33	7.85	2.36	0.13 (1)	0.72
	C. fiber	0	-	-	-	-	-		
	C. californicus	8	7.72	0.85	6.77	9.00	10.94		
MT4MLD	*C. canadensis*	6	8.64	0.25	8.38	9.05	2.87	63.13 (1)	***0.00***
	C. fiber	0	-	-	-	-	-		
	C. californicus	8	10.57	0.55	9.87	11.40	5.20		
MT5L	*C. canadensis*	14	41.23	2.93	33.81	46.28	7.10	5.14 (1)	***0.04***
	C. fiber	0	-	-	-	-	-		
	C. californicus	3	45.33	2.21	43.04	47.45	4.87		

MT5APD	*C. canadensis*	7	5.76	0.28	5.54	6.26	4.92	9.64 (1)	***0.02***
	C. fiber	0	-	-	-	-	-		
	C. californicus	3	6.61	0.62	5.96	7.19	9.35		
MT5MLD	*C. canadensis*	7	5.53	0.43	4.83	6.07	7.84	5.41 (1)	***0.05***
	C. fiber	0	-	-	-	-	-		
	C. californicus	3	6.25	0.49	5.69	6.60	7.81		

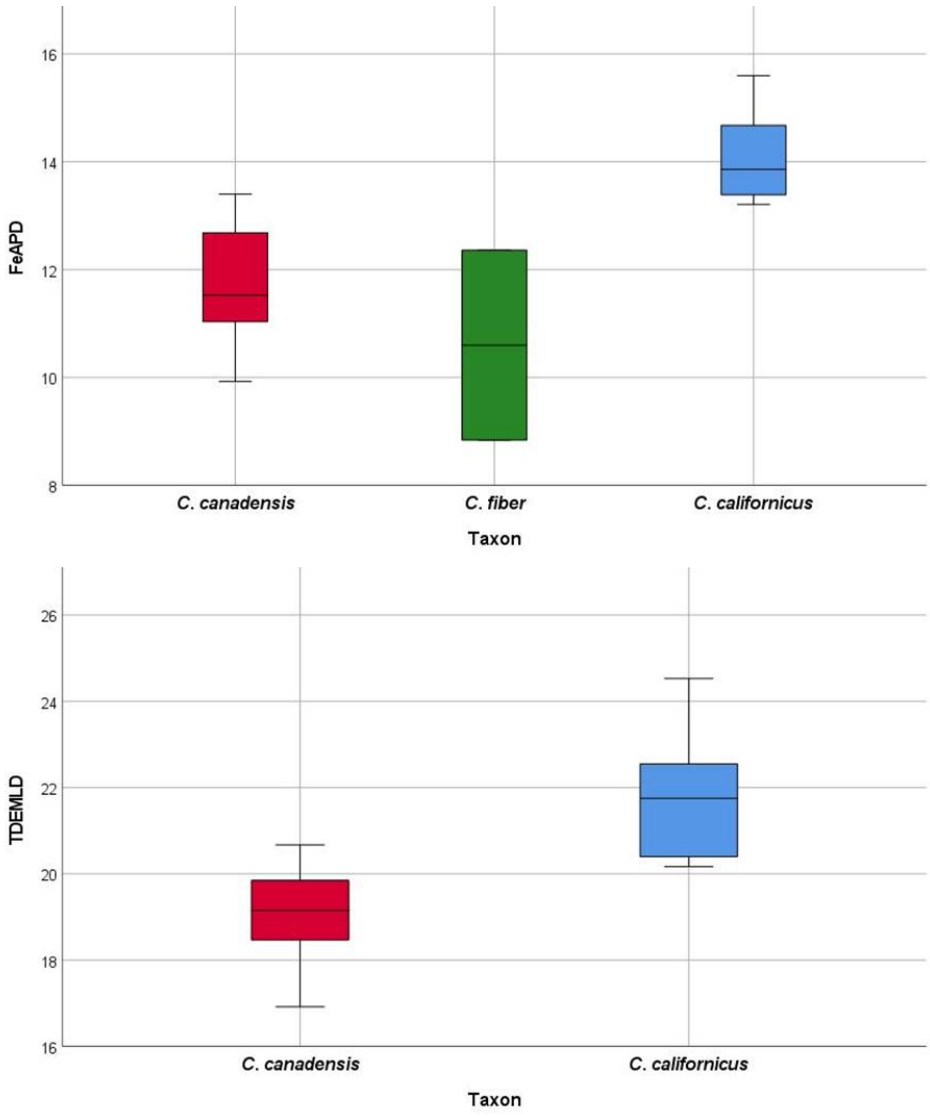

Figure 21. Postcranial elements of *Castor canadensis* and *C. californicus* which exhibit differences in mean values and minimal overlap in range values

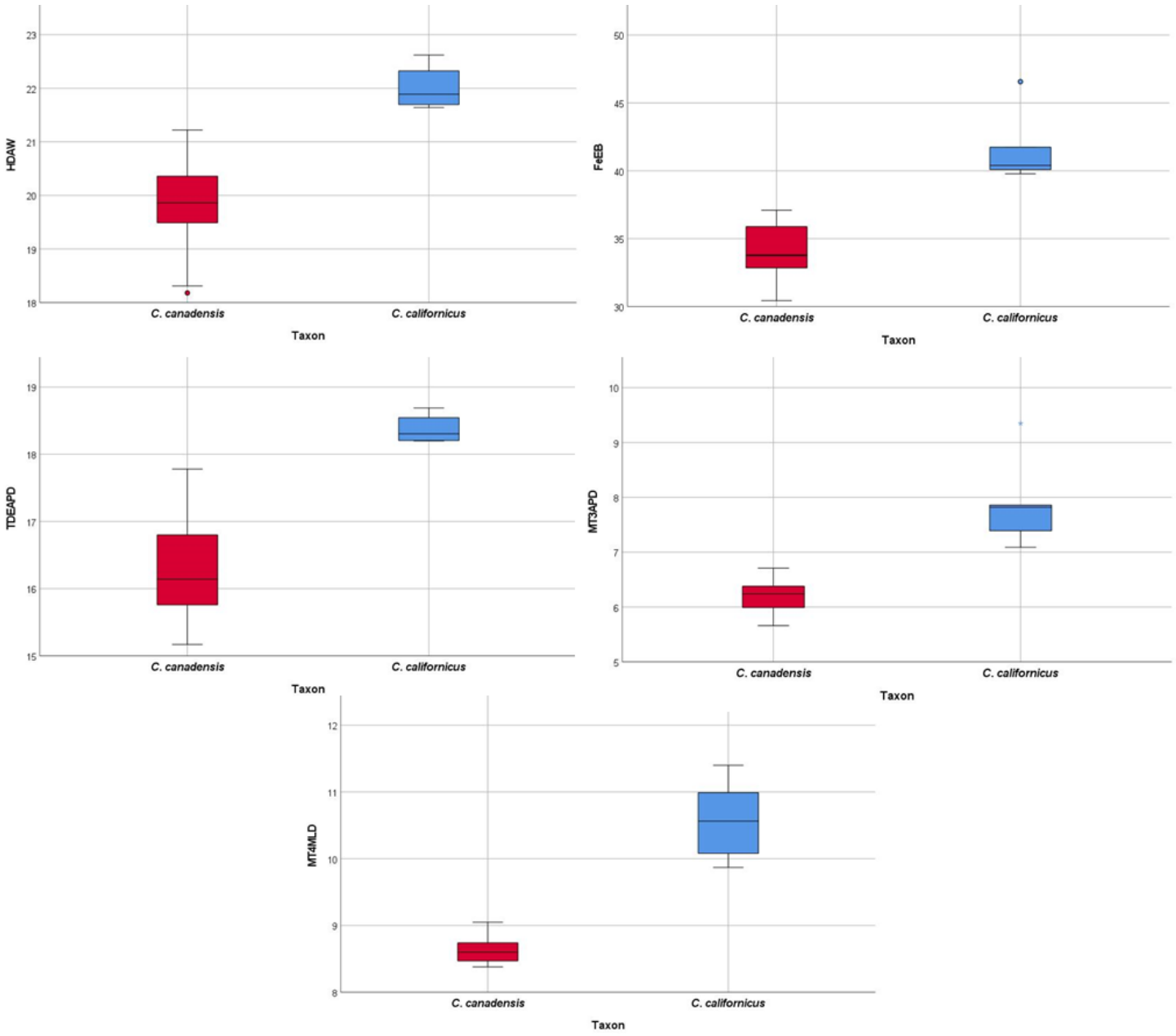

Figure 22. Postcranial elements of *Castor canadensis* and *C. californicus* which exhibit differences in mean values and no overlap in range values

Coefficients of Variation

Coefficients of variation were calculated for measurements with more than three samples per species, which were included with descriptive statistics and ANOVA results in Table 13. Species overall showed high levels of variation between postcranial elements (Figure 23).

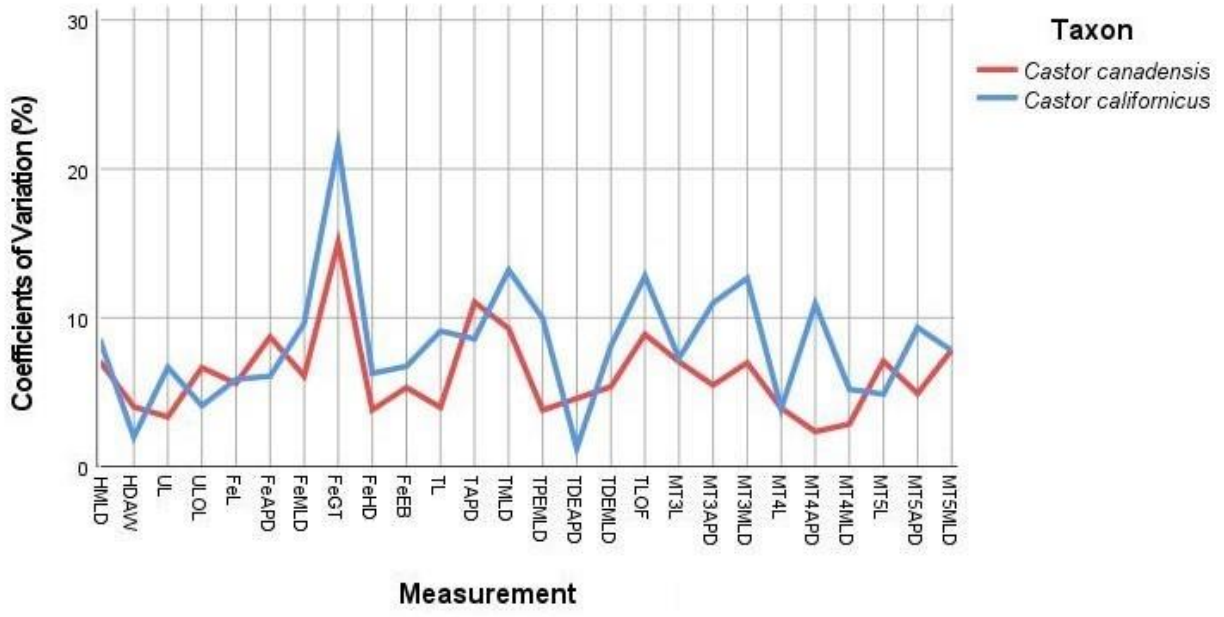

Figure 23. Coefficients of variation calculated for *Castor canadensis* and *C. californicus* postcranial measurements. *C. fiber* removed for clarity

Castor canadensis has good sampling and displays high levels of variation across postcranial measurements. Sampling for metatarsals may be smaller than other elements as museum skeletons may typically lack metapodial elements. *C. californicus* also showed high ranges of variation between measured elements. Variation for both *C. canadensis* and *C. californicus* typically ranged between 3% to 11%, with some elements going as high as 21% and

as low as 1%. Highly variable features, which were not significantly different as determined in the ANOVA, include FeMLD, FeGT, TAPD, TLOF, MT3L, and MT4MLD. The remaining postcranial features also had high ranges of variation and were significantly different based on the ANOVA results. The high ranges of variation are due to inadequate sampling and therefore should not be used as a reliable metric for determining species variation of *C. fiber* in this analysis.

Ecological Niche Modeling

Distribution models of *Castor canadensis* had AUC values between 0.596-0.866 with high commission rates (Table 14). Commission rates indicate the percent of the modeled study area that may be suitable. Modern distribution (using only bioclimatic data), Last Interglacial, Last Glacial Maximum, and 2081-2100 models showed precipitation seasonality (Bio 15) was the most important variable for determining suitable habitat area, closely followed by isothermality (Bio 3), and annual mean temperature (Bio 1) (Table 15). Bioclimatic variable importance was different for the Pliocene projection, as the dataset contained fewer bioclimatic variables than other projections in the analysis. Precipitation seasonality (Bio 15), annual mean temperature (Bio 1), mean temperature of driest quarter (Bio 9), and mean temperature of warmest quarter (Bio 10) were important for determining Pliocene suitability (Table 16).

Table 14. *Castor canadensis* accuracy metrics for climatic variables

	AUC	Commission (%)
Modern (Bioclimatic Variables Only)	0.602	68.1
Modern (Bioclimatic Variables and Ecoregions)	0.757	49.0
Modern (Ecoregions Only)	0.866	31.8
Pliocene	0.596	39.9
Last Interglacial	0.602	33.8
Last Glacial Maximum	0.602	24.5
SSP370 EC-Earth-Veg 2081-2100	0.602	58.7

Table 15. Bioclimatic variables and contributions for *Castor canadensis* modern distribution models. Variables with greater than 10% contribution to the model are listed

Model	Variable	Percent Contribution
WorldClim Bioclimatic Variables	Precipitation Seasonality (Bio 15)	26.8
	Isothermality (Bio 3)	16.3
	Annual Mean Temperature (Bio 1)	11.9
WorldClim Bioclimatic Variables and EPA Level III Ecoregions of North America	Annual Mean Temperature (Bio 1)	44.3
	Isothermality (Bio 3)	19.9
	Mean Temperature of Warmest Quarter (Bio 10)	10
EPA Level III Ecoregions of North America	EPA Level III Ecoregions of North America	100

Table 16. Bioclimatic variables and contributions for *Castor* Pliocene distribution models. Variables with greater than 10% contribution to the model are listed

Model	Variable	Percent Contribution
Pliocene M2	Precipitation Seasonality (Bio 15)	28.9
	Annual Mean Temperature (Bio 1)	17.1
	Mean Temperature of Driest Quarter (Bio 9)	15.5
	Mean Temperature of Warmest Quarter (Bio 10)	10.6

Modern Distribution Models

Habitats for *Castor canadensis* were modeled as suitable through the central portion of North America and extended into portions of Alaska and Mexico (Figure 24A). Areas with low suitability included the northern regions of Canada, Alaska, peninsular Florida, and the southern region of Mexico (Figure 24A).

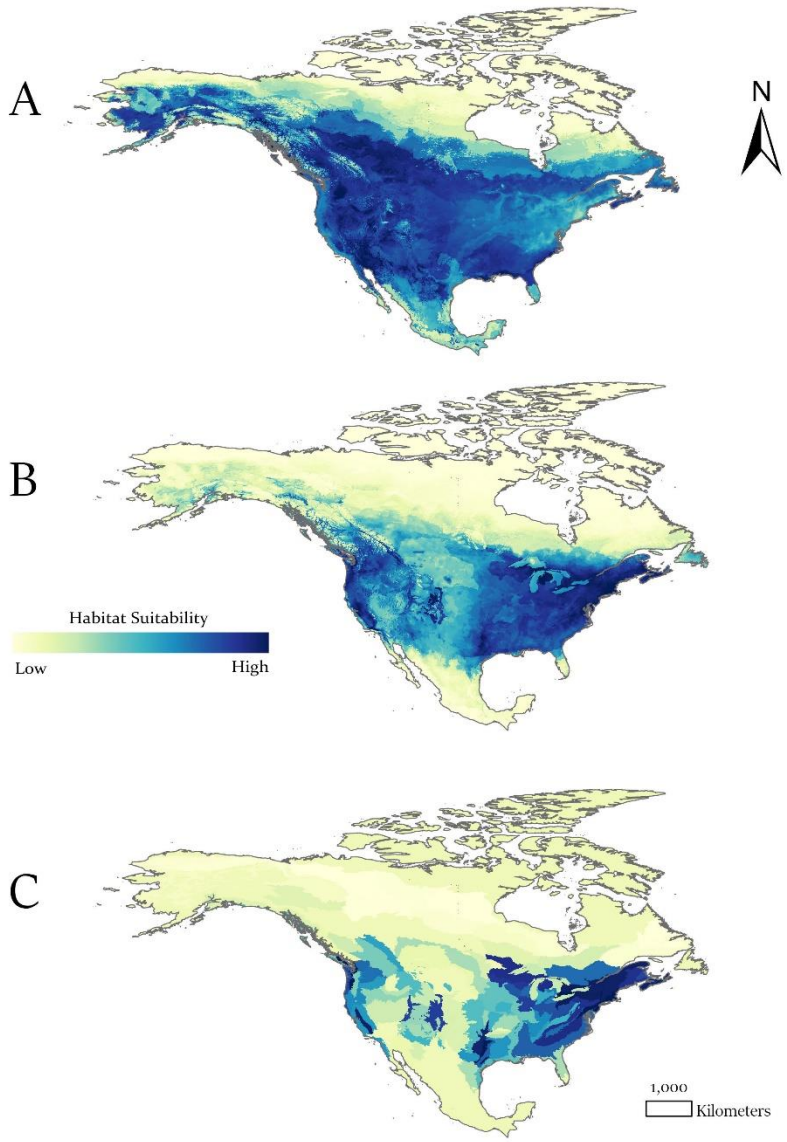

Figure 24. Current distribution models for *Castor canadensis*. (A) Modern distribution model using only bioclimatic variables. (B) Modern distribution model using both bioclimatic variables and EPA Level III ecoregions. (C) Modern distribution model using only EPA Level III ecoregions. Darker blue areas represent a higher probability of habitat suitability while lighter areas represent areas with lower suitability

The model which included the EPA North America Level III Ecoregions and 19 bioclimatic variables had good accuracy metrics when compared to those seen in the model using only the bioclimatic variables (Table 14). Temperature bioclimatic variables were more important to distribution determination in this model compared to the strictly bioclimatic variables model (Table 15). This could be because factors like precipitation are accounted for more by the ecoregions than bioclimatic variables. Northern areas of Canada and Alaska and southern areas of Mexico and peninsular Florida were highly reduced compared to the model using only bioclimatic variables (Figure 24B).

The distribution model using EPA Level III ecoregions had good accuracy metrics when compared to those seen in the model using only the bioclimatic variables (Table 14). Ecoregion data considers multiple factors including climate, vegetation, hydrology, terrain, and land usage (Commission for Environmental Cooperation, 2011). This model predicted the smallest suitable area of the three models (Figure 24C).

Projected Distribution Models

Habitat suitability for *Castor* in North America during the Pliocene (3.3 Ma) was predicted to be suitable in some areas already occupied by *Castor canadensis* today (Figure 25). Most fossil occurrences of *Castor* during the Pliocene lie in areas of high suitability projected by the model (Figure 25A). Areas in the southern latitudes of Mexico and Florida were more suitable in the Pliocene than today (Figure 25B).

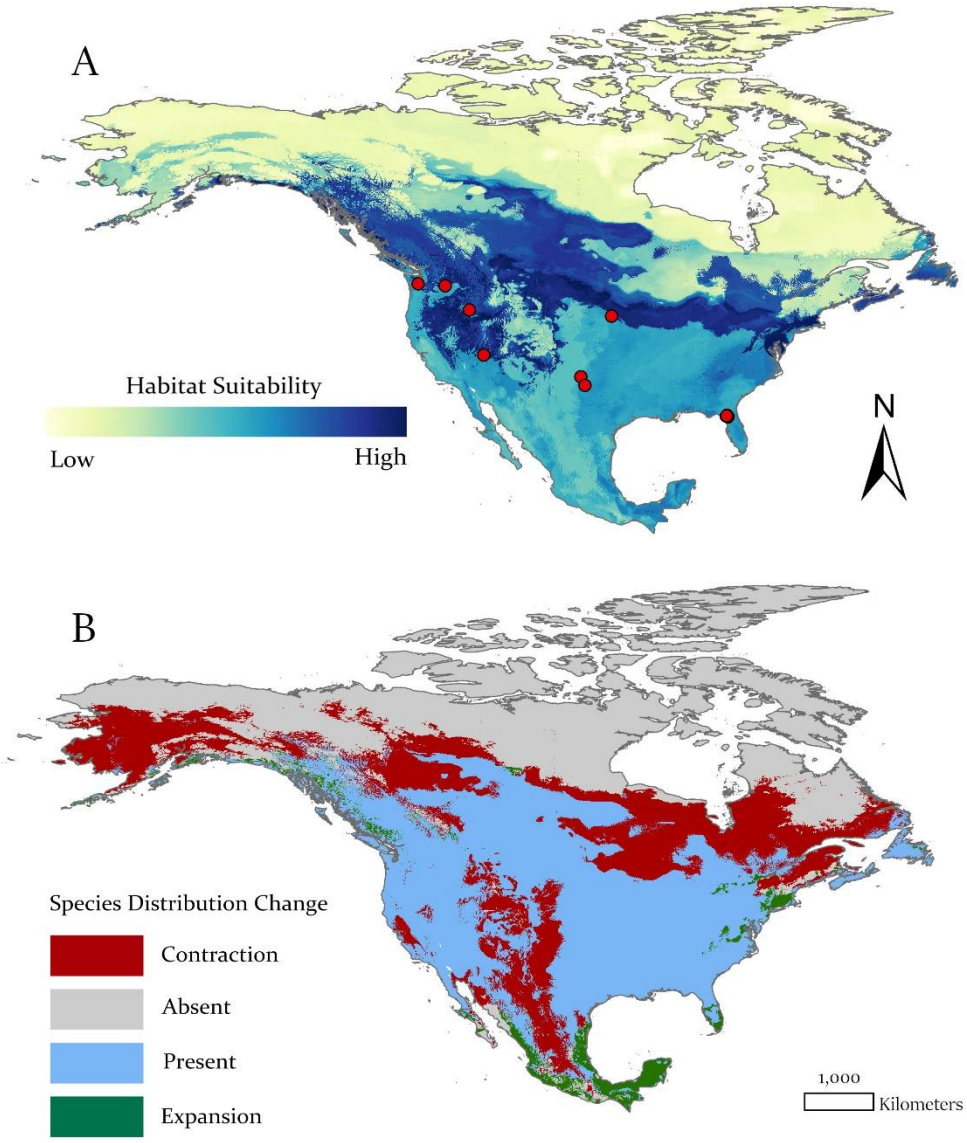

Figure 25. (A) Projected Pliocene distribution model for *Castor* with fossil localities of *Castor californicus* (Appendix D). Darker blue areas represent a higher probability of habitat suitability while lighter areas represent areas with lower suitability. (B) Predicted change of *Castor* distribution from the Pliocene (3.3 Ma) to present

Habitat suitability for the Last Interglacial period (130 ka) was predicted in some areas still occupied by *Castor canadensis* today (Figure 26). All fossil occurrences of *Castor* during the Last Interglacial period lie in areas of high suitability projected by the model (Figure 26A). Southern latitudes significantly increased in suitability during this period, while northern and eastern regions significantly decreased (Figure 26B).

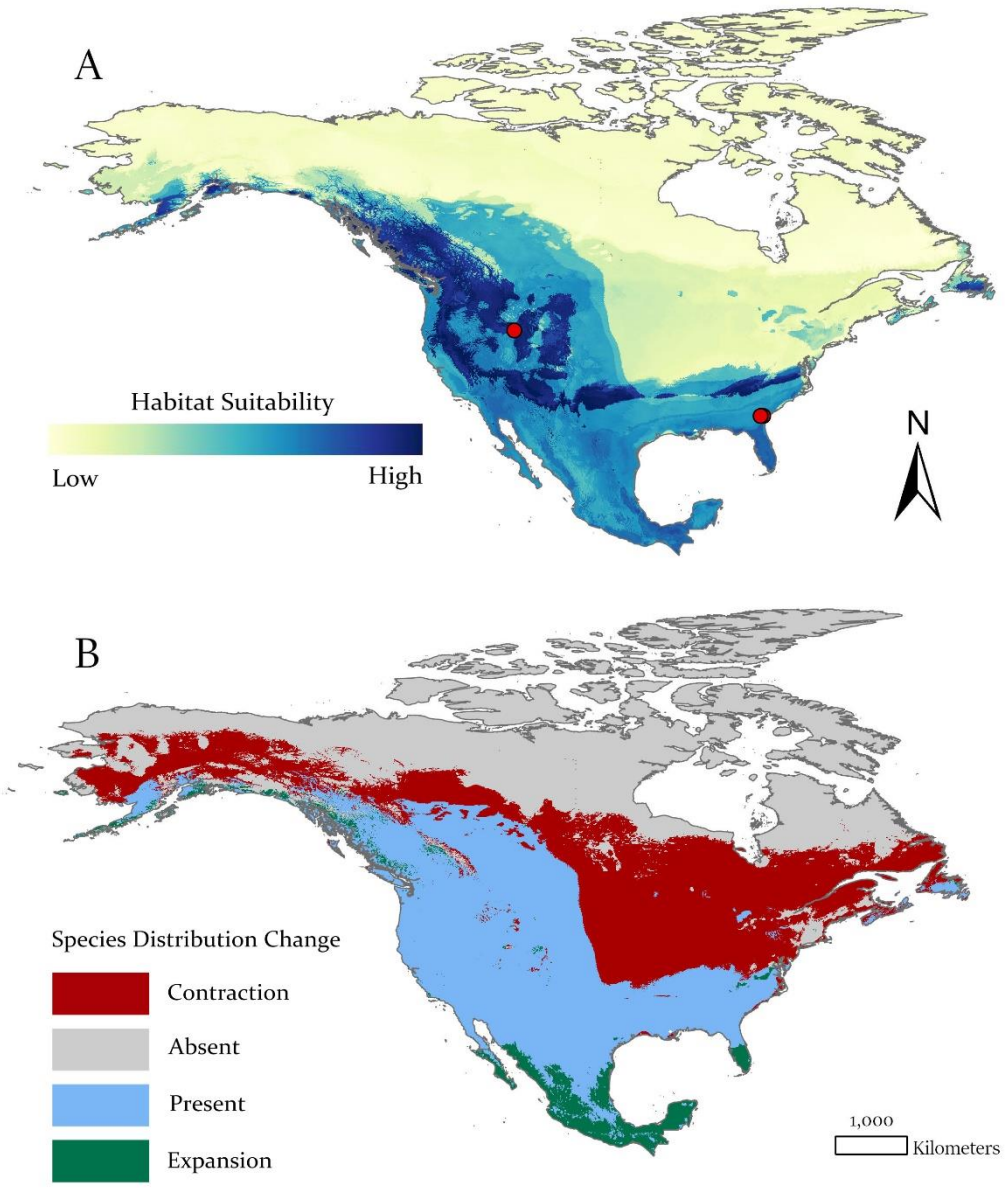

Figure 26. (A) Last Interglacial period projected distribution model for *Castor* with fossil localities of *Castor canadensis* (Appendix E). Darker blue areas represent a higher probability of habitat suitability while lighter areas represent areas with lower suitability. (B) Predicted change of *Castor* distribution from the Last Interglacial period (130 ka) to present

The Last Glacial Maximum (21 ka) model predicted extreme changes in habitat suitability compared to the modern distribution of *Castor canadensis* (Figure 27). Nearly all fossil occurrences of *Castor* during the Last Glacial Maximum lie in areas of high suitability projected by the model (Figure 27A). Glacial extent covered nearly all of Canada and reached into some northern regions of the United States, pushing habitat suitability for *Castor* further south (Figure 27B). Southern regions of North America, particularly Mexico and peninsular Florida, were predicted to be highly suitable.

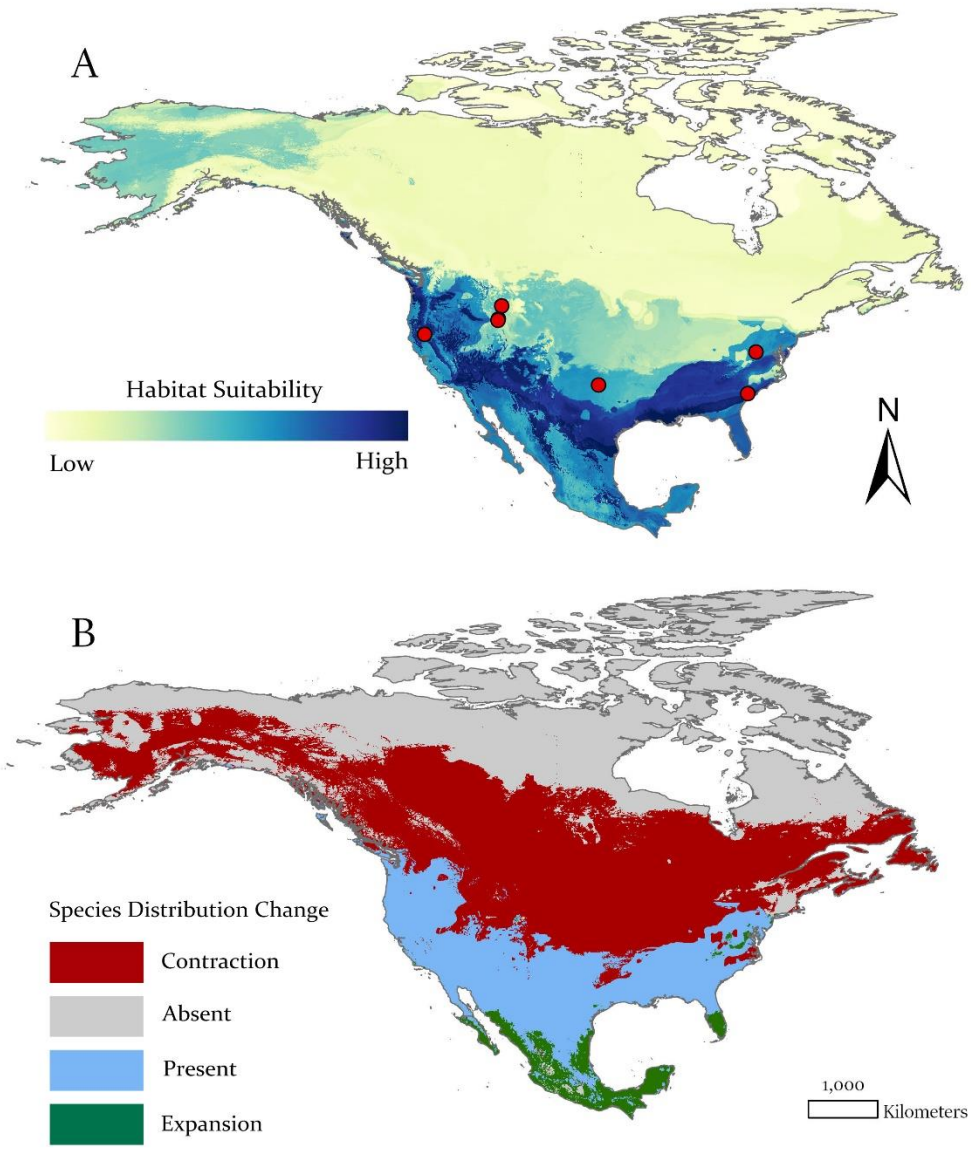

Figure 27. (A) Last Glacial Maximum projected distribution model for *Castor* with fossil localities of *Castor canadensis* (Appendix F). Darker blue areas represent a higher probability of habitat suitability while lighter areas represent areas with lower suitability. (B) Predicted change of *Castor* distribution from the Last Glacial Maximum (21 ka) to present

The future projected distribution model for 2081-2100 showed similar habitat suitability compared those modeled of *Castor canadensis* today (Figure 28A). Areas in the northern latitudes of Canada and Alaska showed higher suitability than previously recorded, while areas of the northern Great Plains, Great Lakes region, and southern latitudes including Mexico and parts of Florida displayed lower suitability (Figure 28B).

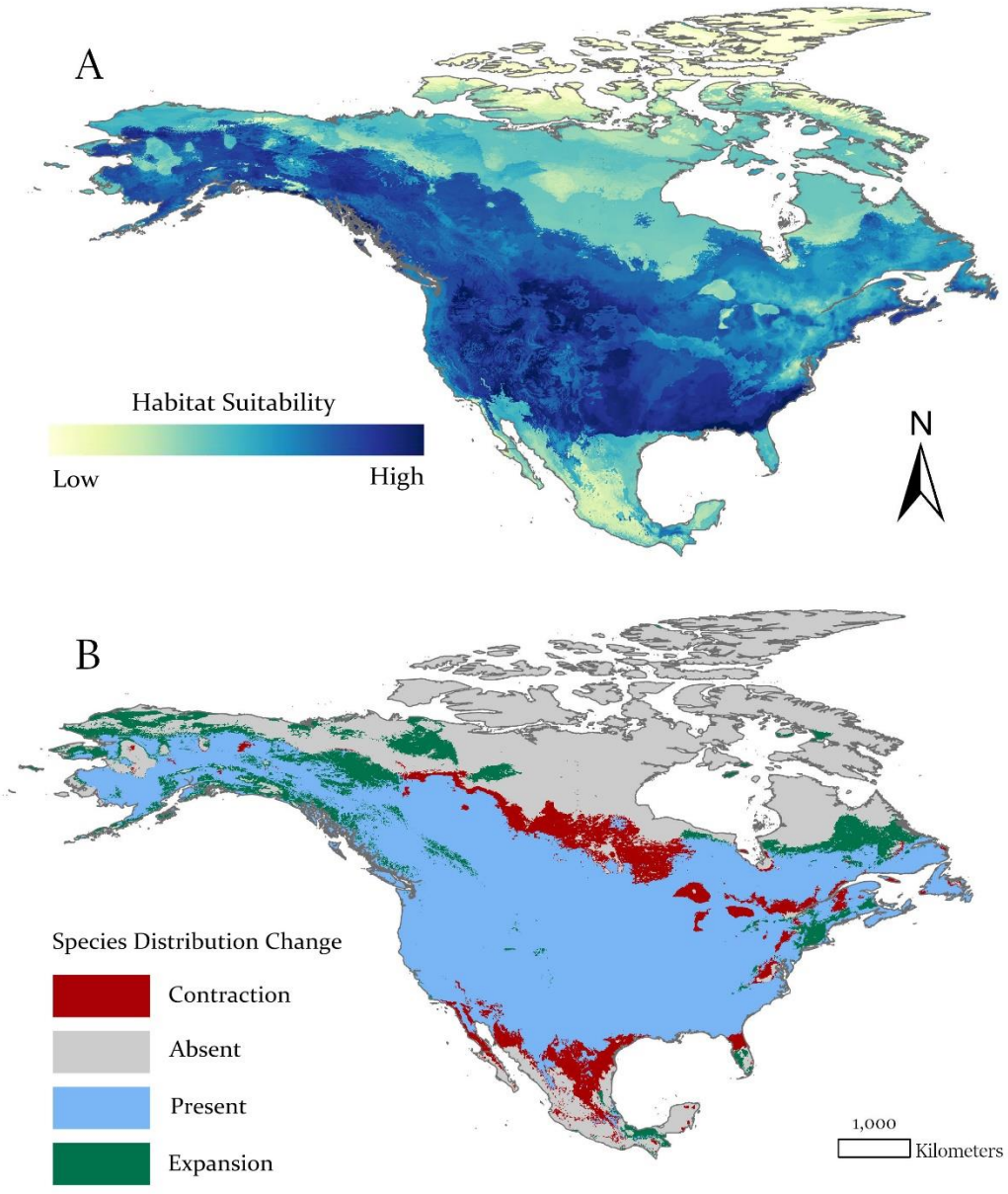

Figure 28. (A) Future (2081-2100) projected distribution model for *Castor canadensis*. Darker blue areas represent a higher probability of species occurrence while lighter areas represent a lower occurrence probability. (B) Predicted change of *Castor* distribution from the present to the future (2081-2100)

CHAPTER 4. DISCUSSION

Geometric Morphometrics

Relative warp analysis of both cranial and dentary material revealed a close association between *Castor canadensis* and *C. californicus*. Dorsal views both show *C. californicus* fitting within the range of morphospace variation for DRW1 and 2 of *C. canadensis* (Figure 6), which are associated with shortened nasals, wide posterior cranium, and posterior positioning of the orbit (Figure 7). Lateral views also show close association between *C. californicus* and *C. canadensis.* All specimens fall in the range of morphospace variation for LRW1 and 3, where one specimen of *C. californicus* fell within the cluster of *C. canadensis* and two specimens fell just outside the morphospace range of *C. canadensis* (Figure 8). The lateral view grouping of *C. californicus* and *C. canadensis* are associated with elongated nasals and shortened posterior cranium between nuchal crest and occipital condyles (Figure 7). Relative warps of the ventral view did not show any clear separation between species, indicating an absence of consistent morphological differences between species in this view (Table 4). *C. canadensis* and *C. californicus* had more morphological distinctions within the dentary. For DenRW1 all three *Castor* species overlap, with *C. canadensis* showing a broad range of variation (Figure 10). Most specimens of *C. californicus* fell outside of the DenRW2 range of *C. canadensis,* with *C. californicus* having a wider separation between the condylar and articular processes and anteroventral positioning of incisor alveolus (Figures 9). Across relative warp analysis *C. fiber* consistently plotted separately from *C. canadensis* and *C. californicus*, showing distinct morphological differences between both extant species.

Canonical variate analysis (CVA) also showed a close association between *C. canadensis* and *C. californicus*. Cranial CVA in which *C. californicus* was classified *a priori* as unknown, one *C. californicus* overlapped with *C. canadensis* and the other was between the two extant species, closer to *C. fiber* (Figure 11), which were characterized to have more shortened nasals, posteromedial positioned orbit, and widening of the posterior cranium (Figure 12). In the classification stage, *C. californicus* had one specimen assigned to *C. canadensis* and one to *C. fiber* (Table 9). When species were all categorized *a priori, C. canadensis* and *C. californicus* did separate into distinct groups fairly well (Figure 14). Along canonical variate one, *C. californicus* was characterized to have elongated nasals, narrowed posterior cranium, and narrowed premaxilla more like *C. fiber*, while with canonical variate two *C. californicus* was associated with shortened nasals and broader posterior cranium like *C. canadensis* (Figure 13). The classification stage did result in one of two specimens of *C. californicus* assigned as *C. canadensis* in cross-validation (Table 10). Dentary CVA, where *C. californicus* was classified as unknown, grouped all *C. californicus* with *C. canadensis* (Figure 15) which are associated with anteroventrally positioned coronoid process, posterior positioning of condylar process, ventral position of angular process, and anterior position of pterygoid insertion (Figure 17). The classification stage primarily categorized *C. californicus* with *C. canadensis* (Table 11). When the dentary CVA had all species classified *a priori, C. californicus* and *C. canadensis* plotted near each other along both canonical variates (Figure 18), where both species displayed anterior positioning of the coronoid process (Figure 17). The classification stage had *C. californicus* classified as *C. canadensis* for one of three specimens (Table 12).

The cluster analysis of cranial and dentary material showed a strong similarity between *C. canadensis* and *C. californicus* (Figure 19). *C. californicus* clustered within the groupings of

C. canadensis cranial specimens, indicating shared morphological similarities between the two species (Figure 19). Dentary specimens showed greater separation between species, with *C. californicus* forming the outgroup from *C. canadensis* and *C. fiber*, suggesting more morphological differences distinguishing the species (Figure 20).

Overall, *Castor canadensis* shows high levels of variation in cranial morphology. The geometric morphometric analysis all resulted in widespread distribution of the species within morphospace. It has been noted in previous literature that *C. canadensis* is highly variable, as at one time it was separated into subspecies based on phenotypic characteristics and regional distribution across North America (Rhoads 1898; Jenkins and Buscher 1979; Long 2000). Specimens of *C. canadensis* used in this study were collected from across North America (Appendices A and B); therefore, the resulting variation seen within the species is a good representation of the variation seen across the continent in the recent past and present.

Castor californicus consistently plotted within the observed range of variation of *C. canadensis* across analyses (Figures 6, 8, and 10). This suggests cranial morphological features are more similar in *C. canadensis* and *C. californicus* than either is with *C. fiber.* Previous studies on the mitochondrial DNA of *Castor canadensis* and *C. fiber* show that the two species last shared a common ancestor as early as 7.5 million years ago (Horn et al. 2011). This timing corresponds with the oldest known record of *C. californicus* in North America from the Rattlesnake Formation in Oregon (Samuels and Zancanella 2011). Cranial morphological similarities between *C. canadensis* and *C. californicus* broadly include shortened nasals, widened posterior cranium, and posterior positioning of the orbit when compared to *C. fiber*. Dentaries of *C. canadensis* and *C. californicus* both display anterior placement of the anterior margin of the pterygoid insertion and widening between the posterior processes. This suggest both North

American species have larger pterygoid muscles than *C. fiber* and broader nuchal region, which is the insertion of the neck muscles.

Postcranial Analysis

Postcranial analysis showed that the range of variation for *C. californicus* fit largely within the range of variation seen for *C. canadensis* (Table 13). The postcranial analysis of *C. fiber* showed high levels of variation for the species. However, this is due to inadequate sampling rather than observable variation. The postcranial elements which were measured did show differences between those of *C. canadensis*, though not enough data was collected to confidently describe and statistically evaluate morphological differences between the two species.

Two elements exhibited significant differences in mean values, while having some overlap in ranges, between *C. canadensis* and *C. californicus*, the anteroposterior diameters of the femur (FeAPD) and mediolateral diameter at the distal end of the tibia (TDEMLD) (Table 13). Five elements showed significant differences in mean values and displayed non-overlapping ranges between *C. canadensis* and *C. californicus,* including the articular width of the humerus at the distal end (HDAW), epicondylar breadth of the femur (FeEB), anteroposterior diameter at the distal end of the tibia (TDEAPD), anteroposterior diameter of the 3rd metatarsal (MT3APD), and mediolateral diameter of the 4th metatarsal (MT4MLD) (Table 13).

Semi-aquatic rodents exhibit a wide range of osteological specializations for their lifestyles (Howell 1930). Characteristics include shortening of the femur, robust limb elements, enlarged muscle attachment sites for the hind limb, and elongated hindfoot to aid in movement through the water (Samuels and Van Valkenburgh 2008). These characteristics hold true for *C. canadensis* and *C. californicus*. The femur anteroposterior diameter (FeAPD) in *C. canadensis* is

low, exhibiting an extreme flattening of the femur while *C. californicus* exhibits a more robust anteroposterior diameter than *C. canadensis* (Figure 21). The femoral epicondylar breadth (FeEB) is wider in *C. californicus* than in *C. canadensis* (Figure 22). A wider FeEB would allow for greater muscle attachments to help with swimming (Samuels and Van Valkenburgh 2008) and would be expected in an animal of larger body mass. The anteroposterior and mediolateral diameters at the distal end of the tibia (TDEAPD and TDEMLD) are slightly wider in *C. californicus* than in *C. canadensis*, suggesting that *C. californicus* had more robust articular distal ends on the hindlimbs than *C. canadensis* (Figure 21 and 22). In the pes, the anteroposterior diameter of the third metatarsal (MT3APD) and mediolateral diameter of the fourth metatarsal (MT4MLD) are both more robust in *C. californicus* than *C. canadensis* (Figure 22). Increasing the size of the pes can aid in increasing the surface area of the hindfoot for increased propulsion through the water (Samuels and Van Valkenburgh 2008), which would also be expected at larger body mass. The articular width at the distal end of the humerus (HDAW) is wider in *C. californicus* than *C. canadensis*, suggesting that *C. californicus* had more robust articular distal ends on the forelimbs than *C. canadensis* (Figure 22), which may allow a wider range of motions and facilitate both swimming and digging.

Castor canadensis and *C. californicus* show high levels of variation in postcranial morphology. Coefficients of variation for both species were highly variable and significantly different (Figure 23 and Table 13), suggesting that differentiating species based on size is not a reliable metric. Previous studies of *C. californicus* described it as closely resembling the extant *C. canadensis* but larger in size (Stirton 1935; Shotwell 1970). As shown in other studies, size is not generally a reliable metric for identifying and distinguishing species (Emery-Wetherell and Davis 2018). Therefore, as *C. canadensis* has high variation within its morphology, size alone

should not be used to distinguish *C. californicus* from *C. canadensis*. Although certain postcranial features showed differences in range between *C. californicus* and *C. canadensis*, most *C. californicus* elements measured in the study fit within the observed range of variation for *C. canadensis*.

Ecological Niche Modeling

Modern habitat suitability for *Castor canadensis*, using only bioclimatic variables, fell into previously recorded distributions (Figure 24). Bioclimatic variables highly contributing to the model included precipitation seasonality, isothermality, and annual mean temperature (Table 15). Predicted distributions, using both bioclimatic variables and ecoregions and only ecoregions, modeled more restricted distributions (Figure 24). Model accuracy, determined from area under the curve (AUC) values produced by MaxEnt, were lower for the model using only bioclimatic variables compared to the higher AUC values produced for the other modern distribution models (Table 14). AUC scores were likely lower for predicting species habitat as *C. canadensis* inhabits a wide range of areas across North America (Figure 1). Previous works studying beaver habitats were conducted at more localized ranges, using variables including stream gradient, watershed size, and hardwood cover in riparian zones (Touihri et al. 2018).

The Pliocene model (3.3 Ma) for *Castor* showed similar ranges of suitability as today, with major restrictions of habitats in the northern and central regions of the continent (Figure 25). Bioclimatic variables highly contributing to the model include precipitation seasonality, annual mean temperature, mean temperature of driest quarter, and mean temperature of warmest quarter (Table 16). Variables affecting the model differ, likely because bioclimatic variables were absent for this dataset. The mid-Pliocene warming period, 3.3- 3.0 Ma, represents a period

where global temperatures were warmer than today (Dowsett and Caballero-Gill 2010; Dolan et al. 2015). However, the Marine Isotope Stage M2 showed a period of cooling, which is represented by the bioclimatic variables used to produce the model (Figure 25) (Dolan et al. 2015). Loss of habitat suitability in the northern and central regions of North America and expansion into coastal and southern regions (Figure 25B) could be attributed to climatic cooling facilitated by the closing of the Isthmus of Panama and opening of the Bering Strait (Brierley and Fedorov 2016).

The Last Interglacial model (130 ka) showed high suitability habitats in the southern and western regions of North America, but low suitability in the far north and eastern regions (Figure 26). Bioclimatic variables highly contributing to the model included precipitation seasonality, isothermality, and mean annual temperature. Although regions in northern and eastern North America are predicted to be less suitable, it is uncertain what factors could be directly impacting this possible contraction in habitat suitability (Figure 26B). Global temperatures during the Last Interglacial period were approximately five degrees warmer than those seen today (Anderson et al. 2004). Recent studies suggest that precipitation seasonality during the Last Interglacial period was more variable, and that seasonal precipitation was lower in some regions of North America (Scussolini et al. 2019). The models produced by Scussolini et al. (2019) correspond with areas predicted to have lower suitability for *Castor*.

Castor distributions were highly restricted during the Last Glacial Maximum (21 ka), particularly in the northern latitudes across the continent (Figure 27). Bioclimatic variables highly contributing to the model included precipitation seasonality, isothermality, and mean annual temperature. Global temperatures during the Last Glacial Maximum were approximately four degrees cooler than today, with continental ice sheets covering much of the northern

latitudes and decreased sea level (Otto-Bliesner et al. 2006). Northern latitudes significantly contract in habitat suitability due to the continental ice sheets extending further south into North America (Figure 27B). Habitats in southern latitudes, in Mexico and peninsular Florida, likely became more suitable as global temperatures cooled by, creating more suitable habitats in previously unsuitable areas of North America.

The future projection model (2081-2100) showed *Castor canadensis* distributed in similar ranges of suitability as today, with major restrictions of habitats in the north-central, south-central, and Great Lakes regions of the continent (Figure 28). The 2081-2100 model used a predicted middle range trajectory climate scenario (EC-Earth-Veg SSP3-7.0) to create bioclimatic variables used for the model. This means that distributions for *C. canadensis* could be predicted as drastically different for best- or worst-case climate scenarios. Northern latitudes, especially eastern and western portions of Canada and Alaska, were predicted to become more suitable (Figure 28). Southern regions, including northern peninsular Florida, north-central Mexico, and northern regions including the Great Lakes and northern Great Plains decreased in suitability (Figure 28). If beavers retreat from these areas of low suitability, that could cause catastrophic effects to water availability, water quality, erosion, and loss of biodiversity (Naiman et al. 1988; Rosell et al. 2005; Pollock et al. 2017; Touihri et al. 2018; Thompson et al. 2020).

Although model predictions do not extend back into the arrival of *Castor* into North America during the Miocene, Pliocene projections into the present can help us understand the expansion of *Castor* throughout the continent. Based on the resulting projection models, habitats in the late Miocene, although not mapped, might have been highly suitable across northwestern portions of North America due to warmer climatic conditions. Warming seen in the Miocene likely opened otherwise low suitable areas in Alaska and western North America, providing

Castor with habitats suitable for their semiaquatic and dam building lifestyles. As climate cooled from the Miocene into the Pliocene, those corridors across the Bering land bridge likely became less suitable for *Castor* and pushed their distributions further south into North America.

The niche models for *Castor* distributions across North America showed distinct shifts in habitat suitability from the Pliocene to the present. Fossil occurrences of both *Castor californicus* and *C. canadensis* fell within suitable habitat ranges predicted in the distribution models (Figures 25A, 26A, and 27A). This suggests that the environmental requirements and distributions for *C. californicus* are like those of *C. canadensis*, as would be expected given the strong morphological similarity between the two taxa.

Overview

Overall, cranial, dentary, and postcranial morphology of *Castor californicus* has been shown to be highly similar to *C. canadensis*. The overall morphological similarities between *C. canadensis* and *C. californicus* likely indicate similarities in diet and locomotor ecology, which would highly suggest the two species are ecologically analogous. Notable cranial morphological differences in *C. californicus* include widened posterior cranium and posterior positioning of orbit. Dentary morphology in *C. californicus* was distinct with wider separation between condylar and articular processes and anteroventral position of incisor alveolus. Postcranial morphology of *C. californicus* had less dorsoventral flattening of the femur, increased hindlimb robustness, and increased metatarsal widths, representing some noticeable differences from extant species of *Castor*. These differences are likely a consequence of anagenetic changes in a species over several million years, with *C. californicus* being ancestral to *C. canadensis*.

Castor distribution and habitat suitability expands and contracts throughout North America from the Pliocene to today. Pliocene distributions show fewer suitable habitats in the northern and central regions of the continent likely due to cooling, while southern regions become more favorable. Last Interglacial distributions show massive reductions in habitat suitability in the northern and eastern regions, likely from warming temperatures and changes in seasonal precipitation. Distribution in the Last Glacial Maximum show massive reduction in distribution in northern and central North America due to continental ice sheet extent. Fossil occurrences of *Castor* in North America fall within the high suitability regions projected by the models. This suggests that *C. californicus* and *C. canadensis* have similar habitat requirements and ecological needs, further asserting that the two species are analogs.

Future directions to further evaluate species validity might include looking in detail at dental dimensions and occlusal patterns and evaluate how they change ontogenetically. This would allow to more confidently comment on the validity of species, or whether they represent chronospecies. Other studies might consider DNA testing to understand the relationship and timing of divergence between members of the genus *Castor* and sampling for isotopes to identify preferences in diet and habitat.

CHAPTER 5. CONCLUSION

Through this analysis of cranial and postcranial material, *Castor californicus* has been shown to be highly similar to the extant North American beaver, *C. canadensis*. Some differences between *C. californicus* and other members of the genus *Castor* are present including wider posterior cranium, wider separation between condylar and articular processes, less dorsoventral flattening of the femur, and increased hindlimb and pes robustness. These differences are likely a consequence of allometry, increased body size, or morphological change in a lineage over several million years. Based on the morphological similarities between the two species, assuming similar ecological roles, both for diet and locomotor ecology, is reasonable. Fossil occurrences of *Castor* in North America coincide with projected habitat suitability for *Castor* from the Pliocene to the present. This suggests that species have similar requirements in habitat and ecological needs, further asserting similarities between the two species. Based on these morphological and environmental factors, *C. canadensis* likely arose from antigenic change within *C. californicus*. However, further work is still needed before reconsidering the taxonomic classifications of these species.

REFERENCES

Anderson KK, Azuma N, Barnola JM, Bigler M, Biscaye P, Caillon N, Chappellaz J, Clausen HB, Dahl-Jensen D, Fischer H, Fluckiger J, et al. 2004. High-resolution record of Northern Hemisphere climate extending into the Last Interglacial period. Nature. 431(7005): 147-151. doi:10.1038/nature02805.

Botkin DB, Saxe H, Araujo MB, Betts R, Bradshaw RHW, Cedhagen T, Chesson P, Dawson TP, Etterson JR, Faith DP, et al. 2007. Forecasting the effects of global warming on biodiversity. BioScience. 57(3):227–236. doi:10.1641/b570306.

Brazier RE, Puttock A, Graham HA, Auster RE, Davies KH, Brown CML. 2020. Beaver: Nature's ecosystem engineers. WIREs Water. 8(1). doi:10.1002/wat2.1494.

Brierley CM, Fedorov AV. 2016. Comparing the impacts of Miocene–Pliocene changes in inter-ocean gateways on climate: Central American Seaway, Bering Strait, and Indonesia. Earth and Planetary Science Letters. 444:116–130. doi:10.1016/j.epsl.2016.03.010.

Brown JL, Bennett JR, French CM. 2017. SDMtoolbox 2.0: the next generation Python-based GIS toolkit for landscape genetic, biogeographic and species distribution model analyses. PeerJ. 5:e4095. doi:10.7717/peerj.4095.

Brown JL, Hill DJ, Dolan AM, Carnaval AC, Haywood AM. 2018. PaleoClim, high spatial resolution paleoclimate surfaces for global land areas. Scientific Data. 5(1). doi:10.1038/sdata.2018.254.

Davis EB, McGuire JL, Orcutt JD. 2014. Ecological niche models of mammalian glacial refugia show consistent bias. Ecography. 37:1133-1138. doi:10.1111/ecog.01294.

Dolan AM, Haywood AM, Hunter SJ, Tindall JC, Dowsett HJ, Hill DJ, Pickering SJ. 2015. Modelling the enigmatic Late Pliocene Glacial Event - Marine Isotope Stage M2. Global and Planetary Change. 128:47–60. doi:10.1016/j.gloplacha.2015.02.001.

Dolin EJ. 2011. Fur, fortune, and empire: the epic history of the fur trade in America. New York; London: W.W. Norton.

Dowsett HJ, Caballero-Gill RP. 2010. Pliocene climate. Stratigraphy. 7(2-3):106–110.

EC-Earth Consortium (EC-Earth). 2019. EC-Earth-Consortium EC-Earth3-Veg model output prepared for CMIP6 ScenarioMIP. Version 2022/04/13. Earth System Grid Federation. doi.org/10.22033/ESGF/CMIP6.727.

Emery-Wetherell M, Davis E. 2018. Dental measurements do not diagnose modern artiodactyl species: Implications for the systematics of Merycoidodontoidea. Palaeontologia Electronica. doi:10.26879/748.

Fick SE, Hijmans RJ. 2017. WorldClim 2: new 1-km spatial resolution climate surfaces for global land areas. International Journal of Climatology. 37(12):4302–4315. doi:10.1002/joc.5086

Flynn LJ, Jacobs LL. 2008. Castoroidea. pp. 391–405. In: Janis CM, Gunnell GF, Uhen MD, eds. Evolution of Tertiary Mammals of North America Volume 2: Small Mammals, Xenarthrans, and Marine Mammals. Cambridge, Cambridge University.

GBIF. 2021. GBIF.org Occurrence Download [dataset]. [accessed 2021 Nov 7]. doi.org/10.15468/dl.jyw9gn.

Hall ER. 1981. The mammals of North America. New York: Wiley.

Hay OP. 1927. The Pleistocene mammals of the Western Region of North America and its Vertebrated Animals. Publication, Carnegie Institute Washington 322B, 346pp.

Howell AB. 1930. Aquatic mammals; their adaptations to life in the water. New York, Dover Publications.

Hugueney M. 1999. Family Castoridae. In: Rössner GE, Heissig K, Josep Antoni Alcover. 1999. The Miocene land mammals of Europe. München: F. Pfeil.

Horn S, Durka W, Wolf R, Ermala A, Stubbe A, Stubbe M, Hofreiter M. 2011. Mitochondrial genomes reveal slow rates of molecular evolution and the timing of speciation in beavers (*Castor*), One of the Largest Rodent Species. Murphy WJ, editor. PLoS ONE. 6(1):e14622. doi:10.1371/journal.pone.0014622.

Jenkins SH, Busher PE. 1979. *Castor canadensis*. Mammalian Species.(120):1. doi:10.2307/3503787.

Karger DN, Nobis MP, Normand S, Graham CH, Zimmermann NE. 2021 May 3. CHELSA-TraCE21k v1.0. Downscaled transient temperature and precipitation data since the last glacial maximum. Climate of the Past Discussions.:1–27. doi:10.5194/cp-2021-30.

Kellogg L. 1911. A fossil beaver from the Kettleman Hills, California. Berkeley: University of California Press.

Korth WW. 1994. The Tertiary record of rodents in North America. New York; London: Plenum.

Kurtén B, Anderson E. 1980. Pleistocene mammals of North America. New York: Columbia University Press.

Long K. 2000. Beaver: a wildlife handbook. Boulder, Co: Johnson Books.

McGuire JL, Davis EB. 2014. Conservation paleobiogeography: the past, present and future of species distributions. Ecography. 37:1092-1049. doi:10.1111/ecog.01337

Martin LD, Bennett D. 1977. The burrows of the Miocene beaver *Palaeocastor*, Western Nebraska, U.S.A. Palaeogeography, Palaeoclimatology, Palaeoecology, 22(3): 173–193..

Martin LD. 1989. Plio-Pleistocene rodents in North America. In: Black CC, Dawson MR (eds.) Papers on fossil rodents in honor of Albert Elmer Wood. Science Series 33. Natural History Museum of Los Angeles County, Los Angeles, CA.

Monteiro LR, Bonato V, dos Reis SF. 2005. Evolutionary integration and morphological diversification in complex morphological structures: mandible shape divergence in spiny rats (Rodentia, Echimyidae). Evolution Development. 7(5):429–439. doi:10.1111/j.1525-142x.2005.05047.x.

Müller-Schwarze D. 2011. The Beaver. Cornell University Press.

Naiman RJ, Johnston CA, Kelley JC. 1988. Alteration of North American streams by beaver. BioScience. 38(11):753–762. doi:10.2307/1310784.

Otto-Bliesner BL, Brady EC, Clauzet G, Tomas R, Levis S, Kothavala Z. 2006. Last glacial maximum and Holocene climate in CCSM3. Journal of Climate. 19(11):2526–2544. doi:10.1175/jcli3748.1.

Otto-Bliesner BL, Marshall SJ, Overpeck JT, Miller GH, Hu A, CAPE Last Interglacial Project Members. 2006. Simulating arctic climate warmth and icefield retreat in the last interglaciation. Science. 311(5768):1751–1753. doi:10.1126/science.1120808.

Peck SB. 2006. Distribution and biology of the ectoparasitic beaver beetle *Platypsyllus castoris* Ritsema in North America (Coleoptera: Leiodidae: Platypsyllinae). Insecta Mundi.85–94.

Pollock MM, Lewallen GM, Woodruff K, Jordan CE, Castro JM. 2017. The beaver restoration guidebook: working with beaver to restore streams, wetlands, and floodplains. Portland, Oregon: U.S. Fish and Wildlife Service.

Rhoads SN. 1898. Contributions to a revision of the North American beavers, otters and fishers. Transactions of the American Philosophical Society. 19(3):417. doi:10.2307/1005498.

Robertson RA, Shadle AR. 1954. Osteologic criteria of age in beavers. Journal of Mammalogy. 35(2):197. doi:10.2307/1376033.

Rosell F, Bozer O, Collen P, Parker H. 2005. Ecological impact of beavers *Castor fiber* and *Castor canadensis* and their ability to modify ecosystems. Mammal Review. 35(3-4):248–276. doi:10.1111/j.1365-2907.2005.00067.x.

Rohlf FJ. 2011. tpsRegr, shape regression, version 1.40. Department of Ecology and Evolution, State University of New York at Stony Brook.

Rohlf FJ. 2015. The tps series of software. Hystrix, the Italian Journal of Mammalogy. 1-4. doi:10.4404/hystrix-26.1-11264.

Rohlf FJ. 2015. tpsRelw: relative warps analysis. Department of Ecology and Evolution, State University of New York at Stony Brook.

Rohlf FJ. 2021. tpsDig2, version 2.31. Department of Ecology and Evolution, State University of New York at Stony Brook.

Rybczynski N. 2007. Castorid phylogenetics: Implications for the evolution of swimming and tree-exploitation in beavers. Journal of Mammalian Evolution. 14(1):1–35. doi:10.1007/s10914-006-9017-3.

Rybczynski N, Ross EM, Samuels JX, Korth WW. 2010. Re-evaluation of *Sinocastor* (Rodentia: Castoridae) with implications on the origin of modern beavers. PLoS ONE. 5(11):e13990. doi:10.1371/journal.pone.0013990.

Samuels JX, Van Valkenburgh B. 2008. Skeletal indicators of locomotor adaptations in living and extinct rodents. Journal of Morphology. 269(11):1387–1411. doi:10.1002/jmor.10662

Samuels JX, Valkenburgh BV. 2009. Craniodental adaptations for digging in extinct burrowing beavers. Journal of Vertebrate Paleontology. 29(1):254–268. doi:10.1080/02724634.2009.10010376.

Samuels JX, Zancanella J. 2011. An early Hemphillian occurrence of *Castor* (Castoridae) from the Rattlesnake Formation of Oregon. Journal of Paleontology. 85(5):930–935. doi:10.1666/11-016.1.

Scussolini P, Bakker P, Guo C, Stepanek C, Zhang Q, Braconnot P, Cao J, Guarino MV, Coumou D, Prange M, et al. 2019. Agreement between reconstructed and modeled boreal precipitation of the Last Interglacial. Science Advances. 5(11). doi: 10.1126/sciadv.aax7047

Shotwell JA. 1970. Pliocene mammals of Southeast Oregon and adjacent Idaho. Bulletin of the Museum of Natural History, University of Oregon 17:1–103.

Stirton RA. 1935. A review of the Tertiary beavers. Berkeley, Calif. Univ. Of California Press.

Thompson S, Vehkaoja M, Pellikka J, Nummi P. 2020 Oct. Ecosystem services provided by beavers Castor spp. Mammal Review. doi:10.1111/mam.12220.

Touihri M, Labbé J, Imbeau L, Darveau M. 2017. North American beaver (*Castor canadensis* Kuhl) key habitat characteristics: review of the relative effects of geomorphology, food

availability and anthropogenic infrastructure. Écoscience. 25(1):9–23. doi:10.1080/11956860.2017.1395314.

Warren DL, Seifert SN. 2011. Ecological niche modeling in Maxent: the importance of model complexity and the performance of model selection criteria. Ecological Applications. 21(2):335–342. doi:10.1890/10-1171.1.

Wright JP, Jones CG, Flecker AS. 2002. An ecosystem engineer, the beaver, increases species richness at the landscape scale. Oecologia. 132(1):96–101. doi:10.1007/s00442-002-0929-1.

Zakrzewski RJ. 1969. The rodents from the Hagerman local fauna, Upper Pliocene of Idaho. Ann Arbor, Museum of Paleontology, University of Michigan.

Zelditch ML, Swiderski DL, Sheets HD, Fink WL. 2004. Geometric morphometrics for biologists: a primer. Amsterdam; Boston: Elsevier Academic Press.

APPENDICES

Appendix A: Cranial Specimens used in Geometric Morphometric Analysis

Catalog Number	Species
ETVP10283	*Castor canadensis*
ETVP11661	*Castor canadensis*
ETVP12488	*Castor canadensis*
ETVP13487	*Castor canadensis*
ETVP14013	*Castor canadensis*
ETVP2224	*Castor canadensis*
ETVP3239	*Castor canadensis*
ETVP33	*Castor canadensis*
ETVP35	*Castor canadensis*
ETVP5012	*Castor canadensis*
ETVP5013	*Castor canadensis*
ETVP5014(1)	*Castor canadensis*
ETVP5014(2)	*Castor canadensis*
ETVP7374	*Castor canadensis*
FMNH1537	*Castor fiber* (fossil)
HAFO2243	*Castor californicus* (fossil)
IVPPOV1105	*Castor fiber*
LACM030104	*Castor canadensis*
LACM10066	*Castor canadensis*
LACM52467	*Castor canadensis*
LACM54561	*Castor canadensis*
LACM54561	*Castor canadensis*
LACM54562	*Castor canadensis*
LACM74973	*Castor canadensis*
LACM85427	*Castor canadensis*
LACM85428	*Castor canadensis*
LACM85429	*Castor canadensis*
LACM85430	*Castor canadensis*
LACM93327	*Castor canadensis*
LACM93329	*Castor canadensis*
LACM93330	*Castor canadensis*
LACM93332	*Castor canadensis*
LACM93333	*Castor canadensis*
LACM93334	*Castor canadensis*

LACM93335	*Castor canadensis*
LACM93336	*Castor canadensis*
LACM93337	*Castor canadensis*
LACM9848	*Castor canadensis*
MVZ183809	*Castor canadensis*
MVZ19229	*Castor fiber*
MVZ210	*Castor canadensis*
MVZ4225	*Castor canadensis*
MVZ52041	*Castor canadensis*
MVZ52048	*Castor canadensis*
MVZ52052	*Castor canadensis*
MVZ52056	*Castor canadensis*
MVZ52639	*Castor canadensis*
MVZ62831	*Castor canadensis*
MVZ80744	*Castor canadensis*
MVZ84568	*Castor canadensis*
MVZ84890	*Castor canadensis*
MVZ84891	*Castor canadensis*
MVZ90873	*Castor canadensis*
USNM174938	*Castor fiber*
USNM248154	*Castor fiber*
UCLA13102	*Castor canadensis*
UCLA17854	*Castor canadensis*
UCLA9516	*Castor canadensis*
UCLA9517	*Castor canadensis*
UCLA9519	*Castor canadensis*
UCLA9521	*Castor canadensis*
UCLA9522	*Castor canadensis*
UCLA9560	*Castor canadensis*
UCLA9561	*Castor canadensis*
UCLA9798	*Castor canadensis*
UCLA9799	*Castor canadensis*
UF22520	*Castor californicus* (fossil)
USNM26154	*Castor californicus* (fossil)

Appendix B: Dentary Specimens used in Geometric Morphometric Analysis

Catalog Number	Species
ETVP10283	*Castor canadensis*
ETVP11661	*Castor canadensis*
ETVP12495	*Castor canadensis*
ETVP12498	*Castor canadensis*
ETVP12500	*Castor canadensis*
ETVP13487	*Castor canadensis*
ETVP14013	*Castor canadensis*
ETVP35	*Castor canadensis*
ETVP5013	*Castor canadensis*
ETVP5014	*Castor canadensis*
ETVP7374	*Castor canadensis*
LACM030104	*Castor canadensis*
LACM074971	*Castor canadensis*
LACM10066	*Castor canadensis*
LACM52467	*Castor canadensis*
LACM54561	*Castor canadensis*
LACM54562	*Castor canadensis*
LACM85427	*Castor canadensis*
LACM85429	*Castor canadensis*
LACM93327	*Castor canadensis*
LACM93329	*Castor canadensis*
LACM93330	*Castor canadensis*
LACM93332	*Castor canadensis*
LACM93333	*Castor canadensis*
LACM93334	*Castor canadensis*
LACM93335	*Castor canadensis*
LACM9848	*Castor canadensis*
MVZ4225	*Castor canadensis*
MVZ52041	*Castor canadensis*
MVZ52056	*Castor canadensis*
MVZ80744	*Castor canadensis*
MVZ84568	*Castor canadensis*
MVZ84890	*Castor canadensis*
MVZ84891	*Castor canadensis*
MVZ90873	*Castor canadensis*
USNM174938	*Castor fiber*

USNM248154	*Castor fiber*
UF22520	*Castor californicus* (fossil)
UO16338	*Castor accessor* (fossil)
USNM26154	*Castor californicus* (fossil)

Appendix C: Postcranial Specimens and Measurements

Catalog Number	Species	Collection Locality	Age	ScaL	ScaW	ScaAL	HL	HAPD
AMNH 154	*Castor canadensis*		Holocene	87.50	41.40	27.96	83.85	11.75
AMNH 155	*Castor canadensis*		Holocene	82.09	39.11	30.01	81.75	12.40
AMNH 156	*Castor canadensis*		Holocene	78.14	40.25	28.82	81.65	11.42
AMNH 157	*Castor canadensis*		Holocene	82.73	43.07	28.00	84.84	13.78
AMNH 158	*Castor canadensis*		Holocene	76.79	36.43	30.51	80.38	10.83
AMNH 159	*Castor canadensis*		Holocene	84.72	40.36	29.27	85.61	11.80
AMNH 160	*Castor canadensis*		Holocene	81.24	45.88	30.98	82.30	11.57
AMNH 161	*Castor canadensis*		Holocene	73.46	38.52	30.07	79.69	12.25
AMNH 162	*Castor canadensis*		Holocene	87.18	45.42	32.17	59.50	12.45
AMNH 163	*Castor canadensis*		Holocene	80.25	36.01	27.29	82.95	10.43
AMNH 164	*Castor canadensis*		Holocene	78.28	36.68	29.85	81.96	11.09
AMNH 165	*Castor canadensis*		Holocene	85.00	36.45	29.24	81.30	11.62
AMNH 166	*Castor canadensis*		Holocene	81.78	42.52	29.71	78.64	11.51
AMNH 167	*Castor canadensis*		Holocene	74.36	39.81	26.88	77.42	11.68
AMNH 168	*Castor canadensis*		Holocene				81.95	12.22
AMNH 169	*Castor canadensis*		Holocene	69.34	35.97	26.51	76.01	10.00
AMNH 170	*Castor fiber*		Holocene				63.30	7.90
ETVP 10285	*Castor canadensis*	Trenton, NE	Holocene	94.19	40.06	27.94	85.18	13.25
ETVP 10286	*Castor canadensis*	Trenton, NE	Holocene	86.52	41.56	26.89	85.38	13.63
ETVP 10480	*Castor canadensis*	Trenton, NE	Holocene					

Catalog Number	Species	Collection Locality	Age	ScaL	ScaW	ScaAL	HL	HAPD
ETVP 10484	*Castor canadensis*	Trenton, NE	Holocene					
ETVP 11658	*Castor canadensis*		Holocene	89.44	38.32	28.59	87.02	13.94
ETVP 2223	*Castor canadensis*	Navajo County, AZ	Holocene				86.06	12.70
ETVP 387	*Castor canadensis*		Holocene	79.29	41.60	26.77	84.60	11.26
HAFO 2329	*Castor californicus*	Hagerman Local Fauna, ID	mid Blancan				90.30	13.58
HAFO FS05-50	*Castor californicus*	Hagerman Local Fauna, ID	mid Blancan					13.05
IMNH 12411	*Castor sp.*	Birch Creek, ID	late Blancan					
IMNH 23534	*Castor californicus*	Hagerman Local Fauna, ID	mid Blancan					
IMNH 32924	*Castor californicus*	Hagerman Local Fauna, ID	mid Blancan					
IMNH 32925	*Castor californicus*	Hagerman Local Fauna, ID	mid Blancan					
IMNH 33610	*Castor californicus*	Hagerman Local Fauna, ID	mid Blancan					
IMNH 33611	*Castor californicus*	Hagerman Local Fauna, ID	mid Blancan					
IMNH 33629	*Castor californicus*	Hagerman Local Fauna, ID	mid Blancan					
IMNH 34464	*Castor californicus*	Hagerman Local Fauna, ID	mid Blancan					
IMNH 34484	*Castor californicus*	Hagerman Local Fauna, ID	mid Blancan					
IMNH 34484	*Castor californicus*	Hagerman Local Fauna, ID	mid Blancan					
IMNH 34506	*Castor californicus*	Hagerman Local Fauna, ID	mid Blancan					
IMNH 34527	*Castor californicus*	Hagerman Local Fauna, ID	mid Blancan					
IMNH 34594	*Castor californicus*	Hagerman Local Fauna, ID	mid Blancan					
IMNH 34604	*Castor californicus*	Hagerman Local Fauna, ID	mid Blancan					
IMNH 34761	*Castor californicus*	Hagerman Local Fauna, ID	mid Blancan					
IMNH 36280	*Castor californicus*	Hagerman Local Fauna, ID	mid Blancan					

Catalog Number	Species	Collection Locality	Age	ScaL	ScaW	ScaAL	HL	HAPD
IMNH 37188	*Castor californicus*	Hagerman Local Fauna, ID	mid Blancan					
IMNH 38176	*Castor californicus*	Hagerman Local Fauna, ID	mid Blancan					
IMNH 38178	*Castor californicus*	Hagerman Local Fauna, ID	mid Blancan					
IMNH 38180	*Castor californicus*	Hagerman Local Fauna, ID	mid Blancan					
IMNH 4841	*Castor californicus*	Hagerman Local Fauna, ID	mid Blancan					
IMNH 4853	*Castor californicus*	Hagerman Local Fauna, ID	mid Blancan					
IMNH 50001	*Castor canandensis*	American Falls Reservoir, ID	Rancholabrean					
IMNH 7851	*Castor californicus*	Hagerman Local Fauna, ID	mid Blancan					
IMNH 7965	*Castor californicus*	Hagerman Local Fauna, ID	mid Blancan					
IMNH 9928	*Castor californicus*	Hagerman Local Fauna, ID	mid Blancan					
KUVP 104070	*Castor canadensis*	Kansas River, Bonner Spring, KS	Pleistocene				80.13	13.90
KUVP 126129	*Castor canadensis*	Kansas River, Bonner Spring, KS	Pleistocene					
KUVP 126359	*Castor canadensis*	Kansas River, Bonner Spring, KS	Pleistocene					
KUVP 86622	*Castor canadensis*	Kansas River, Bonner Spring, KS	Pleistocene					
KUVP 88316	*Castor canadensis*	Kansas River, Bonner Spring, KS	Pleistocene					
KUVP 94596	*Castor canadensis*	Kansas River, Bonner Spring, KS	Pleistocene					
UCMP 32922	*Castor fiber*	Cambridge, UK	Pleistocene			27.96	83.85	11.75

Catalog Number	HMLD	HHD	HDAW	RL	RAPD	RMLD	UL	UAPD	UMLD	ULOL	MC1L
AMNH 154	11.16	17.83	19.22	85.92	7.13	7.30	122.66	12.72	6.65	26.97	7.35
AMNH 155	10.92	17.95	19.68	83.63	7.45	6.69	118.85	12.07	6.77	25.85	6.54
AMNH 156	9.59	19.05	20.10	83.25	5.66	7.65	117.52	12.66	6.87	26.90	7.15
AMNH 157	12.00	18.45	19.74	86.89	7.04	7.07	121.92	12.81	6.47	26.96	7.85
AMNH 158	9.63	17.87	19.80	84.92	7.18	7.38	117.61	11.86	6.40	26.40	6.97
AMNH 159	11.43	17.83	18.94	89.67	7.68	6.56	122.57	12.56	6.14	25.91	7.18
AMNH 160	10.23	18.43	19.28	86.85	7.05	7.71	120.57	14.75	7.61	26.25	8.02
AMNH 161	10.46	18.19	20.06	82.00	7.55	7.19	116.13	12.39	6.96	26.10	7.02
AMNH 162	10.70	19.22	20.36	90.71	7.00	8.35	130.28	14.34	6.46	28.57	
AMNH 163	10.81	17.54	18.18	84.44	6.42	5.15	118.3	10.08	5.56	23.34	
AMNH 164	10.48	18.34	19.86	87.90	6.50	5.14	121.69	10.52	5.43	24.61	
AMNH 165	9.55	17.13	19.67	84.05	6.75	5.05	118.97	11.38	5.76	22.90	
AMNH 166	11.36	18.35	20.66	83.91	7.38	6.24	114.41	12.87	6.23	23.97	7.22
AMNH 167	10.69	17.34	19.88	80.53	6.59	5.59	112.99	10.66	5.89	23.13	
AMNH 168	10.15	17.39	20.69	82.52	6.91	5.38	118.79	10.89	6.12	25.45	
AMNH 169	9.79										
AMNH 170	7.49			59.32	3.97	4.53	85.07	7.13	3.86	16.29	
ETVP 10285	11.90	16.23	21.22	92.07	7.69	6.83	123.10	12.61	6.71	24.41	
ETVP 10286	11.93	17.44	20.95								
ETVP 10480											
ETVP 10484											
ETVP 11658	10.67	18.11	19.49	87.69	5.45	7.99	118.95	12.3	6.91	25.15	
ETVP 2223	10.29	18.47	19.96	93.02	6.29	7.69	125.13	11.59	5.56	26.21	
ETVP 387	11.16	17.51	18.31	87.05	5.71	6.68	117.58	11.52	5.66	22.28	
HAFO 2329	13.38	18.73	22.62	93.76	9.52	7.24	130.64	13.50	8.35	25.04	
HAFO FS05-50	11.27	18.56	22.03	85.62	7.36	5.02	115.01	13.11	5.76	23.30	6.66
IMNH 12411											
IMNH 23534											
IMNH 32924											

Catalog Number	HMLD	HHD	HDAW	RL	RAPD	RMLD	UL	UAPD	UMLD	ULOL	MC1L
IMNH 32925											
IMNH 33610							127.76	15.07	6.97	23.39	
IMNH 33611											
IMNH 33629											
IMNH 34464											
IMNH 34484											
IMNH 34484											
IMNH 34506											
IMNH 34527											
IMNH 34594											
IMNH 34604											
IMNH 34761											
IMNH 36280											
IMNH 37188											
IMNH 38176											
IMNH 38178			21.64								
IMNH 38180											
IMNH 4841											
IMNH 4853											
IMNH 50001											
IMNH 7851	12.28		21.75								
IMNH 7965											
IMNH 9928								12.42	6.13		
KUVP 104070	11.63		20.88								
KUVP 126129											
KUVP 126359							115.09	12.38	6.27	23.27	
KUVP 86622											
KUVP 88316											
KUVP 94596											

Catalog Number	HMLD	HHD	HDAW	RL	RAPD	RMLD	UL	UAPD	UMLD	ULOL	MC1L
UCMP 32922											

Catalog Number	MC2L	MC3L	MC3APD	MC3MLD	MC4L	MC5L	Mph3p	Mph3m	Mph3t	InnomL	IllL
AMNH 154	16.34	22.39	3.39	4.45	20.36	13.87	12.47	11.65		177.74	90.06
AMNH 155	15.96	22.92			20.9	12.67					
AMNH 156	15.17	22.7			20.66	12.57					
AMNH 157	16.95	23.22			21.23	12.85					
AMNH 158	15.32	22.83			20.07	13.32				156.63	79.94
AMNH 159	15.61	21.75			19.8	13.7					
AMNH 160	14.3	19.21			20.48	12.74					
AMNH 161	15.69	22.79			20.21	13.14					
AMNH 162											
AMNH 163											
AMNH 164											
AMNH 165		19.66	3.56	3.91			10.27	8.82	14.68	155.66	81.41
AMNH 166	12.73	19.87			17.26	10.23					
AMNH 167											
AMNH 168											
AMNH 169											
AMNH 170											
ETVP 10285											
ETVP 10286											
ETVP 10480										175.13	89.12
ETVP 10484										147.94	70.5
ETVP 11658										176.1	81.21
ETVP 2223											
ETVP 387		18.89	3.43	4.79							
HAFO 2329										220.91	110.65

Catalog Number	MC2L	MC3L	MC3APD	MC3MLD	MC4L	MC5L	Mph3p	Mph3m	Mph3t	InnomL	IllL
HAFO FS05-50	17.48	23.37	3.86		20.35	14.65	10.82	9.28	15.16		
IMNH 12411											
IMNH 23534											
IMNH 32924											
IMNH 32925											
IMNH 33610											
IMNH 33611											
IMNH 33629											
IMNH 34464											
IMNH 34484											
IMNH 34484											
IMNH 34506											
IMNH 34527											
IMNH 34594											
IMNH 34604											
IMNH 34761											
IMNH 36280											
IMNH 37188											
IMNH 38176											
IMNH 38178											
IMNH 38180											
IMNH 4841											
IMNH 4853											
IMNH 50001											
IMNH 7851											
IMNH 7965											
IMNH 9928											
KUVP 104070											
KUVP 126129											

Catalog Number	MC2L	MC3L	MC3APD	MC3MLD	MC4L	MC5L	Mph3p	Mph3m	Mph3t	InnomL	IllL
KUVP 126359											
KUVP 86622											
KUVP 88316											
KUVP 94596											
UCMP 32922											

Catalog Number	FeL	FeAPD	FeMLD	FeGT	FeHD	FeEB	TL	TAPD	TMLD	TPEAPD	TPEMLD
AMNH 154	102.10	12.84	25.65	13.99	17.10	32.88	131.92	16.38	13.75	24.64	32.87
AMNH 155	98.88	11.56	24.17	12.25	16.76	33.04	129.73	15.65	12.83	23.85	31.76
AMNH 156	99.28	11.39	25.74	11.20	17.24	34.56	131.65	15.50	13.61	24.11	34.20
AMNH 157	102.22	12.20	26.05	12.98	17.80	33.64	131.38	16.43	15.67	24.46	33.19
AMNH 158	96.73	10.12	24.55	12.12	16.32	32.75	132.14	14.26	12.83	24.15	33.46
AMNH 159	103.97	11.47	25.42	12.72	17.43	33.92	136.75	16.84	11.05	24.25	32.88
AMNH 160	99.91	11.49	26.39	13.04	16.13	32.85	132.92	16.30	13.08	24.41	31.66
AMNH 161	96.22	11.17	25.16	10.44	17.02	33.04	125.74	15.28	12.73	24.20	33.01
AMNH 162	110.81	12.62	27.77	14.12	17.41	35.25	142.91	17.03	15.02	25.10	35.50
AMNH 163	94.52	9.93	23.75	10.27	17.33		133.72	13.42	11.86	23.25	31.10
AMNH 164	96.60	11.24	23.11	12.40	17.29	34.96	135.78	13.89	12.05	22.91	32.56
AMNH 165	95.93	10.54	21.18	12.81	16.10	32.47	130.76	13.45	13.09	20.53	31.11
AMNH 166	92.71	10.70	24.47	11.54	17.09	36.60	128.81	13.99	12.76	23.27	33.87
AMNH 167	93.68	10.63	24.45	11.64	17.61	32.58	120.76	13.46	13.08	21.69	30.94
AMNH 168	96.54	12.14	25.01	15.62	16.69	31.68	132.01	14.12	10.74	24.19	31.04
AMNH 169	89.44	10.90	23.71				119.75	14.12	13.53		
AMNH 170	69.08	8.84	16.30								
ETVP 10285											
ETVP 10286											
ETVP 10480											
ETVP 10484											

Catalog Number	FeL	FeAPD	FeMLD	FeGT	FeHD	FeEB	TL	TAPD	TMLD	TPEAPD	TPEMLD
ETVP 11658	105.66	11.44	26.45	16.25	16.98	36.08	131.90	12.13	13.89	27.05	32.53
ETVP 2223	108.49	12.86	24.85	18.07	19.22	36.15	134.96	11.02	11.75	26.24	31.95
ETVP 387	103.96	13.40	23.65	16.93	17.12	35.69	130.88	14.80	13.20	27.74	33.29
HAFO 2329	117.267		29.33	19.35	21.40	46.57	156.97	14.28	17.41		38.99
HAFO FS05-50	98.70	13.96	23.73	19.36	20.36	40.09	131.08	12.40	16.17	27.54	32.14
IMNH 12411		14.48	25.60								
IMNH 23534		13.21	25.27								
IMNH 32924											
IMNH 32925											
IMNH 33610	110.24	15.6	31.05	14.01	21.55	41.74					
IMNH 33611											
IMNH 33629		14.31	27.14								
IMNH 34464											
IMNH 34484	113.48			12.32	18.15						
IMNH 34484		13.76	27.52								
IMNH 34506								13.62	13.28		
IMNH 34527											
IMNH 34594		13.26	23.13								
IMNH 34604											
IMNH 34761											
IMNH 36280	106.88	15.04	25.28		20.24	39.79	149.19	15.24	13.62		
IMNH 37188		13.52	26.55								
IMNH 38176											
IMNH 38178											
IMNH 38180				14.71							
IMNH 4841	112.37			11.98	19.47	40.40				24.98	37.55
IMNH 4853											
IMNH 50001	109.69	13.29	27.94	14.34		37.10					
IMNH 7851											

Catalog Number	FeL	FeAPD	FeMLD	FeGT	FeHD	FeEB	TL	TAPD	TMLD	TPEAPD	TPEMLD
IMNH 7965											
IMNH 9928											
KUVP 104070											
KUVP 126129	97.80	13.34	26.61	12.74	16.99	35.89					
KUVP 126359											
KUVP 86622	93.56	12.44	23.41	12.84	17.20	30.44					
KUVP 88316	101.94	12.16	24.78	12.91	17.57	36.30					
KUVP 94596	103.42	12.75	24.30	11.70		32.93					
UCMP 32922	86.78	12.36	27.26								

Catalog Number	TDEAPD	TDEMLD	TLOF	FibL	FibAPD	FibMLD	CalcL	CalcTL	MT1L	MT1APD
AMNH 154	16.28	17.74	41.9	126.5	4.93	4.67	52.57	31.61	27.45	4.62
AMNH 155	15.97	18.71	40.51	122.48	4.76	4.29			27.58	4.61
AMNH 156	16.06	20.67	37.57	124.7	5.55	4.09			27.57	4.18
AMNH 157	16.51	19.85	40.53	127.09	5.58	4.16			28.9	4.13
AMNH 158	17.18	19.22	45.48	125.79	6.45	3.48			27.32	4.1
AMNH 159	16.18	18.82	43.7	132.12	4.72	3.96			30.24	
AMNH 160	16.1	18.47	43.37	126.16	5.14	4.45			28.24	
AMNH 161	15.76	19.41	34.02	120.12	4.68	3.66			27.14	
AMNH 162	16.8	19.61	44.95	137.05	6.18	4.29			28.83	
AMNH 163	15.52	17.96	38.81	127.92	4.53	3.81			23.82	
AMNH 164	16.75	19	35.16	131.25	3.96	3.52				
AMNH 165	15.17	17.86	40.67	124.18	4.18	3.05	46.42	26.73		
AMNH 166	15.92	19.95	41.65	122.77	3.97	3.85			25.83	
AMNH 167	15.73	20.66	33.94							
AMNH 168	15.54	16.92	39.9	128.51	3.02	3.41			27.83	
AMNH 169										
AMNH 170										

Catalog Number	TDEAPD	TDEMLD	TLOF	FibL	FibAPD	FibMLD	CalcL	CalcTL	MT1L	MT1APD
ETVP 10285										
ETVP 10286										
ETVP 10480										
ETVP 10484										
ETVP 11658	17.78	19.15	35.28	124.62	3.57	5.35	48.34	28.19		
ETVP 2223	17.52	19.15	41.48	128.97	4.4	4.66				
ETVP 387	17.39	20.22	40.73	125.23	3.57	3.92	51.91	30.28		
HAFO 2329		24.53	42.71							
HAFO FS05-50			33.18				50.09	25.85	26.13	5.03
IMNH 12411										
IMNH 23534										
IMNH 32924										
IMNH 32925										
IMNH 33610									30.24	4.85
IMNH 33611										
IMNH 33629										
IMNH 34464	18.2	21.75								
IMNH 34484	18.21	22.55								
IMNH 34484										
IMNH 34506										
IMNH 34527										
IMNH 34594										
IMNH 34604	18.69	20.4								
IMNH 34761										
IMNH 36280			36.8				57.8	33.91		
IMNH 37188										
IMNH 38176	18.4	20.17								
IMNH 38178										
IMNH 38180										

Catalog Number	TDEAPD	TDEMLD	TLOF	FibL	FibAPD	FibMLD	CalcL	CalcTL	MT1L	MT1APD
IMNH 4841										
IMNH 4853										
IMNH 50001										
IMNH 7851										
IMNH 7965										
IMNH 9928										
KUVP 104070										
KUVP 126129										
KUVP 126359										
KUVP 86622										
KUVP 88316										
KUVP 94596										
UCMP 32922										

Catalog Number	MT1MLD	MT2L	MT2APD	MT2MLD	MT3L	MT3APD	MT3MLD	MT4L	MT4APD
AMNH 154	4.48	43.58	4.22	5.45	47.62	5.78	6.65	55.20	7.59
AMNH 155	4.14	42.55	4.75	5.47	47.88	6.20	7.27	56.50	7.85
AMNH 156	3.83	42.27	4.18	5.47	50.16	6.27	8.02	58.28	7.69
AMNH 157	4.16	43.06	4.57	5.15	59.76	6.45	7.25	57.68	7.62
AMNH 158	3.43	42.48	4.12	5.08	50.35	6.71	7.77	58.72	7.33
AMNH 159		42.66			50.61			59.05	
AMNH 160		42.56			48.81			56.21	
AMNH 161		42.62			48.29			57.81	
AMNH 162		47.37			52.8			60.78	
AMNH 163		41.75			46.68			52.76	
AMNH 164									
AMNH 165					48.21	5.66	7.40		
AMNH 166		40.49			46.43			55.19	

Catalog Number	MT1MLD	MT2L	MT2APD	MT2MLD	MT3L	MT3APD	MT3MLD	MT4L	MT4APD
AMNH 167									
AMNH 168		39.56			45.35			54.74	
AMNH 169					45.59				
AMNH 170									
ETVP 10285									
ETVP 10286									
ETVP 10480									
ETVP 10484									
ETVP 11658		40.49	4.58	5.31	47.97	6.21	8.16	54.55	7.47
ETVP 2223									
ETVP 387		41.21	4.7	5.54	48.1	6.31	8.12		
HAFO 2329									
HAFO FS05-50	5.22	40.81	4.54	7.11	49.03	7.09	9.88	58.08	7.50
IMNH 12411									
IMNH 23534									
IMNH 32924									7.38
IMNH 32925									6.92
IMNH 33610	5.10	46.57	5.13	6.12		7.86	8.61	62.54	9.00
IMNH 33611								63.52	6.77
IMNH 33629									
IMNH 34464									
IMNH 34484									
IMNH 34484									
IMNH 34506									
IMNH 34527									7.69
IMNH 34594									
IMNH 34604									
IMNH 34761					53.92	7.82	9.95		
IMNH 36280						7.39	9.63	60.73	8.99

Catalog Number	MT1MLD	MT2L	MT2APD	MT2MLD	MT3L	MT3APD	MT3MLD	MT4L	MT4APD
IMNH 37188									
IMNH 38176									
IMNH 38178									
IMNH 38180									
IMNH 4841									
IMNH 4853									7.52
IMNH 50001									
IMNH 7851									
IMNH 7965					56.70	9.35	7.25		
IMNH 9928									
KUVP 104070									
KUVP 126129									
KUVP 126359									
KUVP 86622									
KUVP 88316									
KUVP 94596									
UCMP 32922									

Catalog Number	MT4MLD	MT5L	MT5APD	MT5MLD	Pph3p	Pph3m	Pph3t
AMNH 154	8.74	41.09	6.08	5.25	28.69	14.28	
AMNH 155	8.48	41.80	5.60	4.83			
AMNH 156	8.47	42.58	5.62	6.07			
AMNH 157	8.38	42.79	5.62	5.42			
AMNH 158	9.05	41.96	5.63	5.43			
AMNH 159		43.71					
AMNH 160		42.46					
AMNH 161		42.30					
AMNH 162		46.28					

Catalog Number	MT4MLD	MT5L	MT5APD	MT5MLD	Pph3p	Pph3m	Pph3t
AMNH 163		39.57					
AMNH 164							
AMNH 165					28.98	14.44	17.05
AMNH 166		33.81					
AMNH 167							
AMNH 168		40.42					
AMNH 169							
AMNH 170							
ETVP 10285							
ETVP 10286							
ETVP 10480							
ETVP 10484							
ETVP 11658	8.72	37.59	5.54	5.71			
ETVP 2223							
ETVP 387		40.86	6.26	5.99			
HAFO 2329							
HAFO FS05-50	10.09	43.04	5.96	6.45	28.94	17.50	19.11
IMNH 12411							
IMNH 23534							
IMNH 32924	11.20						
IMNH 32925	9.87						
IMNH 33610	10.65	47.45	6.68	6.60			
IMNH 33611	10.48						
IMNH 33629							
IMNH 34464							
IMNH 34484							
IMNH 34484							
IMNH 34506							
IMNH 34527	10.78						

Catalog Number	MT4MLD	MT5L	MT5APD	MT5MLD	Pph3p	Pph3m	Pph3t
IMNH 34594							
IMNH 34604							
IMNH 34761							
IMNH 36280	10.07	45.49	7.19	5.69	30.68	15.09	18.09
IMNH 37188							
IMNH 38176							
IMNH 38178							
IMNH 38180							
IMNH 4841							
IMNH 4853	11.40						
IMNH 50001							
IMNH 7851							
IMNH 7965							
IMNH 9928							
KUVP 104070							
KUVP 126129							
KUVP 126359							
KUVP 86622							
KUVP 88316							
KUVP 94596							
UCMP 32922							

Appendix D: Pliocene Locality Overlay Data

Site ID	Site Name	Species	Latitude	Longitude	Max Age	Min Age
14407	Cita Canyon [North Cita Canyon]	*Castor californicus*	34.92075	-101.703	4900000	1900000
14418	Haile XV A (Haile 15A)	*Castor californicus*	29.7	-82.5667	4900000	1900000
14424	Meade Locality NO. 10 [Mount Blanco] [TMM 31180]	*Castor californicus*	33.81556	-101.193	4900000	1900000
14428	Panaca Beds, Meadow Valley	*Castor californicus*	37.75	-114.375	4900000	1900000
14435	Santa Fe River 1 (includes 1A & 1B)	*Castor californicus*	29.83333	-82.7833	4900000	1900000
14436	Santa Fe River 15A	*Castor californicus*	29.90833	-82.6667	4900000	1900000
14437	Santa Fe River 4A	*Castor californicus*	29.75	-82.625	4900000	1900000
14439	Santa Fe River 8A	*Castor californicus*	29.875	-82.75	4900000	1900000
14443	Taunton [UWBM Locality A9326]	*Castor californicus*	46.80306	-119.344	4900000	1900000
CP116F	Santee and Devils Nest Airstrip Local Faunas	*Castor californicus*	42.81583	-97.7253	5910000	4910000
PN3C	White Bluffs Local Fauna including Ringold	*Castor californicus*	47.0425	-122.893	4910000	2630000
PN23A	Hagerman Local Fauna	*Castor californicus*	43.61374	-116.238	4910000	2630000

Source 1: Paleobiology Database

Source 2: NOW Database

Appendix E: Last Interglacial Locality Overlay Data

Site ID	Site Name	Species	Latitude	Longitude	Max Age	Min Age
5261	American Falls	*Castor canadensis*	42.75	-112.867	125000	75000
22500	Isle of Hope	*Castor canadensis*	31.98333	-81.6667	130000	71000
26000	Mayfair	*Castor canadensis*	32	-82	130000	71000

Source: Neotoma Database

Appendix F: Last Glacial Maximum Locality Overlay Data

Site ID	Site Name	Species	Latitude	Longitude	Max Age	Min Age
3664	Howard Ranch	*Castor canadensis*	34.36667	-99.75	16775	16775
4419	Merrell [24BE1659]	*Castor canadensis*	44.61667	-112.25	25030	25030
5025	Rainbow Beach [ISUM 72003]	*Castor canadensis*	42.88333	-112.717	33000	21000
5026	Dam Local Fauna [ISUM 52002]	*Castor canadensis*	42.75	-112.75	33000	21000
5782	New Trout Cave	*Castor canadensis*	38.60278	-79.3689	31100	16840
10533	Samwel Cave	*Castor canadensis*	40.9171	-122.232	25605	19063
22641	Ardis	*Castor canadensis*	33.23662	-80.4416	24950	20690

Source: Neotoma Database

VITA

KELLY EILEEN LUBBERS

Education:

M.S. Geosciences, East Tennessee State University, Johnson City, Tennessee, 2022

B.S. Geology, South Dakota School of Mines and Technology, Rapid City, South Dakota, 2018

Public Schools, Libertyville, Illinois, 2014

Professional Experience:

Bonebed Paleontologist, The Mammoth Site of Hot Springs, SD, Inc.; Hot Springs, South Dakota, 2022-Present

Graduate Collections Research Assistant, Gray Fossil Site & Museum; Gray, Tennessee, 2021-2022

Scientists in Parks Paleontology Intern, John Day Fossil Beds National Monument; Kimberly, Oregon, 2021-2021

Graduate Teaching Assistant, East Tennessee State University; Johnson City, Tennessee, 2020-2021

Paleontological Field Technician, Quality Services, Inc.; Rapid City, SD, 2020-2020

Paleontology Field Technician, Environmental Planning Group LLC; Salt Lake City, Utah, 2019-2019

Assistant Education Coordinator, The Journey Museum and Learning Center; Rapid City, SD, 2018-2019

Invertebrate Paleontology Collections Assistant, South Dakota School of Mines and Technology; Rapid City, SD, 2017-2018

CSBR Undergraduate Research Assistant, South Dakota School of Mines and Technology; 2017-2017

Cultural Heritage Curatorial Intern, Keystone Historical Museum; Keystone, SD, 2017-2017

CSBR Undergraduate Research Assistant, South Dakota School of Mines and Technology; 2016-2016

Paleobiology Education Intern, Smithsonian Institution National Museum of Natural History; Washington, DC, 2015-2015

Museum Associate, Museum of Geology; Rapid City, SD 2014-2017

Publications:

Lubbers, Kelly E. and Famoso, Nicholas A. (2021). Occlusal Enamel Complexity of Beavers (Rodentia: Castoroidea) from John Day Fossil Beds National Monument, Oregon: Geological Society of America Abstracts with Programs, v.53, no. 6, doi: 10.1130/abs/2021AM-369835.

Lubbers, Kelly E., Kunza, Lisa., and Mead, Jim I. (2018). Comparative Analysis of Pollen Present at the Mammoth Site, Hot Springs, SD. Abstract submission for South Dakota School of Mines 2018 Student Research Symposium, Undergraduate Oral Presentations.

Honors and Awards:

Mastodon Award, East Tennessee State University, 2021